Resonantly driven wobbling kinks

O. F. Oxtoby*
CSIR Computational Aerodynamics, Building 12, P.O. Box 395, Pretoria 0001, South Africa

I. V. Barashenkov†
Department of Mathematics, University of Cape Town, Rondebosch 7701, South Africa
(Received 4 March 2009; published 31 August 2009)

The amplitude of oscillations of the freely wobbling kink in the ϕ^4 theory decays due to the emission of second-harmonic radiation. We study the compensation of these radiation losses (as well as additional dissipative losses) by the resonant driving of the kink. We consider both direct and parametric driving at a range of resonance frequencies. In each case, we derive the amplitude equations which describe the evolution of the amplitude of the wobbling and the kink's velocity. These equations predict multistability and hysteretic transitions in the wobbling amplitude for each driving frequency—the conclusion verified by numerical simulations of the full partial differential equation. We show that the strongest parametric resonance occurs when the driving frequency equals the natural wobbling frequency and not double that value. For direct driving, the strongest resonance is at half the natural frequency, but there is also a weaker resonance when the driving frequency equals the natural wobbling frequency itself. We show that this resonance is accompanied by the translational motion of the kink.

DOI: 10.1103/PhysRevE.80.026609 PACS number(s): 05.45.Yv

I. INTRODUCTION

The kink of the ϕ^4 equation has a mode of internal oscillation, commonly referred to as the wobbling mode. To check whether the resonant excitation of the wobbling mode could provide a channel for pumping energy into a kink-bearing system, several authors have studied the dynamics of ϕ^4 kinks subjected to resonant direct or parametric driving and damping [1–4]. The damped-driven ϕ^4 theory arises in a variety of physical contexts, in particular in the description of topological-defect dynamics in media with temporally [5] and spatially [6] modulated parameters or in the presence of fluctuations [7]. Examples include the drift of domain walls in ferromagnets in oscillatory magnetic fields [8], the Brownian motion of stringlike objects on a periodically modulated bistable substrate [9], ratchet dynamics of kinks in a lattice of pointlike inhomogeneities [10], and rectification in Josephson junctions and optical lattices [11]. The damped ϕ^4 equation driven by noise was used to study the production of topological defects during the symmetry-breaking phase transition [12] and the spatiotemporal stochastic resonance in a chain of bistable elements [13].

The mathematical analysis of the damped-driven kinks started with the work of Kivshar *et al.* [5] who studied the discrete parametrically pumped ϕ^4 system. Assuming that the driving frequency lies above the phonon band and using the method of averaging, they discovered the phenomenon of kink death for sufficiently large driving strengths. Next, in an influential paper [8], Sukstanskii and Primak considered the continuous ϕ^4 equation with a combination of direct and parametric driving (see also a related discussion in [14]). Using a variant of the Lindstedt-Poincaré technique, where the velocity of the kink is adjusted so as to eliminate secular terms at the lowest orders of the perturbation expansion in powers of the wobbling amplitude, they detected a slow unidirectional motion of the kink. In their analysis, Sukstanskii and Primak were not concerned with terms higher than quadratic in the amplitude of the wobbling; in fact, their approach is not suitable to deal with secular terms at the ϵ^3 order of the expansion — neither can it be utilized in the case of the resonant driving frequency.

The resonant situation was studied by Quintero *et al.* [2–4] who employed the method of projections. The method assumes a specific functional dependence of the kink on the "collective coordinates," which in this case are the width and the position of the kink. Inserting the chosen ansatz in the partial differential equation and projecting the result onto the neutral modes associated with the two degrees of freedom, one obtains a two-dimensional dynamical system, a simplification from the infinite degrees of freedom present in the original partial differential equation. (In the undamped undriven situation, the collective-coordinate approach was pioneered by Rice and Mele [15,16].) The major advantage of the method is that if the collective coordinates have been chosen such that they capture the essentials of the dynamics, one should be able to uncover the very mechanism of the observed nonlinear phenomena—which is otherwise concealed by an infinite number of degrees of freedom (see, e.g., [17]). The drawback of the collective-coordinate approach, however, is that one cannot know beforehand which degrees of freedom are essential and which can be omitted without a qualitative impact on the kink's dynamics. Specifically, the role of radiation (which is neglected in the approach in question) is not obvious and therefore one has no *a priori* guarantee that a radiationless ansatz is adequate. Another disadvantage is that the resulting two-dimensional dynamical system is amenable to analytical study only in a very special case (when the damping is set to zero [2–4]).

*oliver.oxtoby@gmail.com
†igor@odette.mth.uct.ac.za; igor.barashenkov@uct.ac.za

In this paper, we approach the resonantly driven wobbling kink from a complementary perspective. Instead of trying to guess the most pertinent set of collective variables, we construct the wobbler as a singular perturbation expansion using a sequence of space and time scales. The nonsecularity conditions yield equations for the slow-time evolution of the wobbling amplitude and the kink velocity. This asymptotic procedure has already been implemented for the unperturbed ϕ^4 equation [18]; here we extend it to include damping and driving terms. We consider both external (direct) and parametric driving, at several resonant frequencies. This includes the cases considered by Quintero *et al.* in [2–4]. Although the multiscale expansion cannot crystallize the "minimum set" of degrees of freedom accountable for the observed behavior, it does not suffer from the arbitrariness associated with the choice of collective-coordinate ansatz. The multiscale expansion is asymptotic, i.e., only valid for small amplitudes of the wobbling mode; however, in the small-amplitude limit the expansion provides a faithful description of the wobbler, independent of any assumptions and mode preselections. Importantly, it does not neglect the radiation.

In all four cases of the direct and the parametric driving considered in this paper, we derive an autonomous system of equations for the amplitude of the wobbling mode and the velocity of the kink. In each of the four cases, this dynamical system turns out to exhibit stable fixed points corresponding to the nondecaying wobbling of the kink. In some parameter regimes, the amplitude of stable wobbling is nonunique and may undergo hysteretic transitions between two nonzero values. In another case, the wobbling is necessarily accompanied by translational motion of the kink. The conclusions of our asymptotic analysis have been verified in direct numerical simulations of the corresponding partial differential equation. The numerical procedure we shall be using throughout this paper was specified in [18].

An outline of this paper is as follows. In Secs. II and III we study the *parametrically* driven wobbling kink. In Sec. II the frequency of the driver is chosen near the natural wobbling frequency of the kink, while in Sec. III we take the forcing frequency close to double that value. In the next section (Sec. IV), we compare the mechanisms that are at work in each of the two cases. Subsequently, we consider the kink driven *directly*—first near half of its natural wobbling frequency (Sec. V) and then close to the wobbling frequency itself (Sec. VI). Our conclusions are summarized in Sec. VII. Here, in particular, we rank the four resonances according to the amplitude of the resulting stationary wobbling and according to the width of the resonant frequency range.

II. 1:1 PARAMETRIC RESONANCE

A. Asymptotic multiscale expansion

We start with the *parametric* driving of the form

$$\tfrac{1}{2}\phi_{tt} - \tfrac{1}{2}\phi_{xx} + \gamma\phi_t - [1 + h\cos(\Omega t)]\phi + \phi^3 = 0. \quad (1)$$

This type of a driver was previously considered by Quintero *et al.* [4]. The driving frequency Ω is assumed to be slightly detuned from ω_0, the linear wobbling frequency of the undriven kink,

$$\Omega = \omega_0(1 + \rho).$$

We remind the reader that $\omega_0 = \sqrt{3}$ [18]. Introducing a small parameter ϵ (which will be used to measure the amplitude of the wobbling mode in what follows), we choose the detuning in the form

$$\rho = \epsilon^2 R,$$

where R is of order 1. Since the frequency of the free *nonlinear* wobbling is smaller than ω_0 {see Eq. (44) in [18]}, we expect that the strongest resonance will occur not when $\Omega = \omega_0$ but for some small negative ρ. [This will indeed be the case; see Eq. (29) below.]

Next, the parameters $\gamma > 0$ and $h > 0$ are the small damping coefficient and the driving strength, respectively. We choose the following scaling laws for these parameters:

$$\gamma = \epsilon^2\Gamma, \quad h = \epsilon^3 H, \quad (2)$$

where Γ and H are quantities of order 1. This choice of scalings will give rise to amplitude equations featuring the driving term of the same order of magnitude as the linear and the nonlinear damping terms (so that the stationary wobbling regimes become possible). We assume that the kink moves with a slowly varying small velocity $v = \epsilon V$, where $V = V(T_1, T_2, \ldots)$ is of order 1.

Before embarking on the perturbation expansions, we transform Eq. (1) to the comoving reference frame; this gives

$$\frac{1}{2}(1+\rho)^2\phi_{\tau\tau} - v(1+\rho)\phi_{\xi\tau} - \frac{v_\tau}{2}(1+\rho)\phi_\xi - \frac{1-v^2}{2}\phi_{\xi\xi} - \phi + \phi^3 = h\cos(\omega_0\tau)\phi + \gamma v\phi_\xi - \gamma(1+\rho)\phi_\tau. \quad (3)$$

Here

$$\xi = x - \int_0^t v(t')dt'. \quad (4)$$

We have also changed $t \to \tau$, where

$$\Omega t = \omega_0\tau.$$

We now expand the field $\phi(\xi, \tau)$ about the kink $\phi_0 \equiv \tanh\xi$,

$$\phi = \phi_0 + \epsilon\phi_1 + \epsilon^2\phi_2 + \cdots. \quad (5)$$

We also define "slow" space and time variables

$$X_n \equiv \epsilon^n\xi, \quad T_n \equiv \epsilon^n\tau, \quad n = 0,1,2,\ldots,$$

with the standard shorthand notation $\partial_n = \partial/\partial X_n$, $D_n = \partial/\partial T_n$. Substituting Eq. (5) into the ϕ^4 equation (3), making use of the chain-rule expansions $\partial/\partial\xi = \partial_0 + \epsilon\partial_1 + \epsilon^2\partial_2 + \cdots$, $\partial/\partial\tau = D_0 + \epsilon D_1 + \epsilon^2 D_2 + \cdots$, and equating coefficients of like powers of ϵ, we obtain a sequence of linear partial differential equations—just as we have done in the case of the free wobbling [18]. As in the case of the undamped-undriven ϕ^4 equation, the first-order perturbation is chosen to include only the wobbling mode,

$$\phi_1 = A(X_1, \ldots; T_1, \ldots)\,\mathrm{sech}\,X_0\tanh X_0\, e^{i\omega_0 T_0} + \text{c.c.}, \quad (6)$$

while the quadratic correction satisfies the partial differential equation

$$\tfrac{1}{2}D_0^2\phi_2 + \mathcal{L}\phi_2 = F_2(X_0, \ldots; T_0, \ldots) \tag{7}$$

with

$$\mathcal{L} = -\tfrac{1}{2}\partial_0^2 - 1 + 3\phi_0^2 = -\tfrac{1}{2}\partial_0^2 + 2 - 3\ \mathrm{sech}^2 X_0$$

and

$$F_2 = (\partial_0\partial_1 - D_0D_1)\phi_1 - 3\phi_0\phi_1^2 + VD_0\partial_0\phi_1 + \tfrac{1}{2}D_1V\partial_0\phi_0 - \tfrac{1}{2}V^2\partial_0^2\phi_0. \tag{8}$$

As in [18], the second-order perturbation is taken to consist just of the harmonics present in the forcing function (8),

$$\phi_2 = \varphi_2^{(0)} + \varphi_2^{(1)}e^{i\omega_0T_0} + \text{c.c.} + \varphi_2^{(2)}e^{2i\omega_0T_0} + \text{c.c.} \tag{9}$$

Here the coefficient functions $\varphi_2^{(0)}(X_0)$, $\varphi_2^{(1)}(X_0)$, and $\varphi_2^{(2)}(X_0)$ are found by solving the corresponding ordinary differential equations. The solvability condition for the first of these equations is $D_1V=0$ and the solution is

$$\varphi_2^{(0)} = 2|A|^2\mathrm{sech}^2 X_0 \tanh X_0 + \left(\frac{V^2}{2} - 3|A|^2\right)X_0\ \mathrm{sech}^2 X_0 \tag{10}$$

(see [18]). The solution of the last equation is

$$\varphi_2^{(2)} = A^2 f_1(X_0), \tag{11}$$

with

$$f_1(X_0) = \tfrac{1}{8}\{6\tanh X_0\ \mathrm{sech}^2 X_0 + (3 - \tanh^2 X_0 + ik_0\tanh X_0)[J_2^*(X_0) - J_2^\infty]\,e^{ik_0X_0} + (3 - \tanh^2 X_0 - ik_0\tanh X_0)\,J_2(X_0)\,e^{-ik_0X_0}\}. \tag{12}$$

Here the function $J_2(X_0)$ is defined by the integral

$$J_n(X_0) = \int_{-\infty}^{X_0} e^{ik_0\xi}\,\mathrm{sech}^n\xi\,d\xi \quad (k_0 = \sqrt{8}), \tag{13}$$

with $n=2$. The constant J_2^∞ is the asymptotic value of $J_2(X_0)$ as $X_0\to\infty$,

$$J_n^\infty = \lim_{X_0\to\infty} J_n(X_0). \tag{14}$$

Finally, the nonsecularity condition associated with the equation for the coefficient function $\varphi_2^{(1)}(X_0)$ is $D_1A=0$; with this condition in place, the solution $\varphi_2^{(1)}(X_0)$ is bounded for all X_0 and decays as $|X_0|\to\infty$. However, this decay is not fast enough [18]; hence, the term $\varphi_2^{(1)}(X_0)e^{i\omega_0T_0}$ has a *quasi*secular behavior at the infinities and has to be set to zero. This is achieved by imposing the condition [18]

$$\partial_1A + i\omega_0VA = 0. \tag{15}$$

Proceeding to the order ϵ^3, we find the partial differential equation

$$\tfrac{1}{2}D_0^2\phi_3 + \mathcal{L}\phi_3 = F_3, \tag{16}$$

where

$$F_3 = (\partial_0\partial_1 - D_0D_1)\phi_2 + (\partial_0\partial_2 - D_0D_2)\phi_1 + \tfrac{1}{2}(\partial_1^2 - D_1^2)\phi_1 - \phi_1^3 - 6\phi_0\phi_1\phi_2 + VD_0\partial_0\phi_2 + VD_0\partial_1\phi_1 + VD_1\partial_0\phi_1 + \tfrac{1}{2}D_2V\partial_0\phi_0 - \tfrac{1}{2}V^2\partial_0^2\phi_1 - \Gamma D_0\phi_1 + \Gamma V\partial_0\phi_0 - RD_0^2\phi_1 + \tfrac{1}{2}He^{i\omega_0T_0}\phi_0 + \text{c.c.} \tag{17}$$

The cubic correction ϕ_3 consists of harmonics present in the function F_3. The solvability condition for the first harmonic gives the amplitude equation

$$iD_2A + \frac{\omega_0\zeta}{2}|A|^2A - \omega_0\left(R + \frac{V^2}{2}\right)A = \frac{\pi\omega_0}{8}H - i\Gamma A, \tag{18}$$

while the solvability condition for the zeroth harmonic produces

$$D_2V = -2\Gamma V.$$

Letting $a=\epsilon A$ and keeping in mind that $D_1A=0$ and $D_1V=0$, we can rewrite these two equations in terms of the unscaled variables. This gives a system of two master equations:

$$\dot{a} = -\gamma a - i\omega_0\rho a + \frac{i}{2}\omega_0\zeta\,|a|^2a - \frac{i}{2}\omega_0v^2a - i\frac{\pi}{8}\omega_0h + \mathcal{O}(|a|^5), \tag{19a}$$

$$\dot{v} = -2\gamma v + \mathcal{O}(|a|^5), \tag{19b}$$

where the overdots indicate differentiation with respect to t and the complex coefficient ζ was evaluated in [18] as follows:

$$\zeta = \zeta_R + i\zeta_I = -0.8509 + i\,0.04636. \tag{20}$$

B. Reduced two-dimensional dynamics

Since a is complex, Eqs. (19) define a dynamical system in three dimensions. However, Eq. (19b) will damp the variable v until it is of order $|a|^3$ and this will make the term v^2a negligible in Eq. (19a). Thus, after an initial transient, the dynamics will be determined by the two-dimensional system (19a) with $v=0$. Next, the natural wobbling amplitude a may depend, parametrically, on ξ. However, Eq. (15) and the fact that $v\to0$ as t grows imply that a may only depend on ξ via X_2, X_3, etc. That is, the dependence is weak.

Letting $a=re^{-i\theta}$, Eq. (19a) yields

$$\dot{r} = -\frac{\omega_0}{2}\zeta_I\,r^3 + \gamma\,(r_0\sin\theta - r), \tag{21}$$

where $r_0=\frac{\pi}{8}\omega_0h/\gamma$. For all a with $|a|>r_0$, the right-hand side of Eq. (21) is negative and so no trajectories can escape to infinity. On the other hand, applying Dulac's criterion (with Dulac's function equal to a constant), one can easily ascertain that Eq. (19a) with $v=0$ does not have closed orbits. Hence, all trajectories must flow toward fixed points with finite $|a|$.

The fixed points of system (19a) are given by the equation

$$(\gamma + i\omega_0\rho)a - \frac{i\omega_0\zeta}{2}|a|^2 a = -\frac{\pi i\omega_0}{8}h. \tag{22}$$

From Eq. (22), the absolute value of a satisfies

$$\mathcal{H}(|a|^2) = h, \tag{23}$$

where the function $\mathcal{H}(|a|^2)$ is defined by

$$\mathcal{H}^2 = \frac{64}{\pi^2}|a|^2\left[\left(\frac{\gamma}{\omega_0} + \frac{\zeta_I}{2}|a|^2\right)^2 + \left(\rho - \frac{\zeta_R}{2}|a|^2\right)^2\right]. \tag{24}$$

Assume, first, that $\rho > \rho_0$, where

$$\rho_0(\gamma) = \frac{1}{\omega_0}\frac{\zeta_I - \sqrt{3}\zeta_R}{\zeta_R + \sqrt{3}\zeta_I}\gamma = -1.139\gamma. \tag{25}$$

In this case $\mathcal{H}(|a|^2)$ is a monotonically growing function, with the range $(0,\infty)$. Equation (23) has a single positive root $|a|^2$ for any h and the dynamical system (19) has a single stationary point. This fixed point is always stable.

Now let $\rho < \rho_0$. Here, the range of the function $\mathcal{H}(|a|^2)$ is still $(0,\infty)$; however, the function grows for small and large values of $|a|^2$ but decreases in the intermediate interval $|a_-|^2 < |a|^2 < |a_+|^2$, where

$$|a_\pm|^2 = \frac{2}{3}\frac{2\alpha \pm \sqrt{\alpha^2 - 3\beta^2}}{|\zeta|^2}, \tag{26a}$$

$$\alpha = \zeta_R\rho - \zeta_I\frac{\gamma}{\omega_0}, \quad \beta = \zeta_I\rho + \zeta_R\frac{\gamma}{\omega_0}. \tag{26b}$$

Consequently, Eq. (23) has a single root for small and large values of h and three roots in the intermediate region defined by $h_+ < h < h_-$, where

$$h_\pm = \mathcal{H}(|a_\pm|^2). \tag{27}$$

For the dynamical system (19) this implies that there is only one fixed point (which is stable) for small and large h, but as h approaches the value h_+ from below or the value h_- from above, two new fixed points are born in a saddle-node bifurcation. The region $h_+ < h < h_-$ is characterized by bistability; an adiabatic variation of h will result in hysteretic transitions between two stable fixed points.

The existence of hysteresis has been verified in the direct numerical simulations of Eq. (1), with $\gamma = 0.01$. Starting with $h = 0$ we increased h, past h_-, and then reduced it back to zero. At each h step, we used the final values of $\phi(x)$ and $\phi_t(x)$ from the previous-step simulation as initial conditions for the new run. For each h we measured the value of a to which the numerical solution settled after transients died out. The resulting amplitude $|a|$ is shown in Fig. 1; clearly visible is the hysteresis loop. Figure 1 corresponds to simulations with $\rho = -0.03$; for $\rho = -0.02$ the hysteresis loop is smaller and for $\rho = -0.01$ it disappears completely. This is consistent with the value of ρ_0 given by Eq. (25). The value $h_- = 0.008$ at which the amplitude was recorded to jump from the bottom to the top branch in Fig. 1 and the value $h_+ = 0.005$ at which it dropped back as h was decreased are also in agreement with the corresponding predictions of the amplitude equation. Namely, Eqs. (24), (26), and (27) give $h_- = 8.2 \times 10^{-3}$ and $h_+ = 4.9 \times 10^{-3}$.

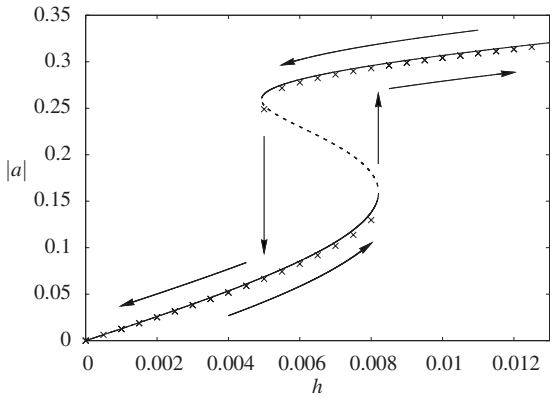

FIG. 1. The hysteresis loop observed in the 1:1 parametrically driven ϕ^4 equation [Eq. (1)] with $\gamma = 0.01$ and $\rho = -0.03$. The driving strength h is increased from 0 to 0.0125 in increments of 5×10^{-4} and then reduced back to 0 as indicated by arrows. Crosses mark simulations of the Eq. (1); continuous and dashed lines depict stable and unstable fixed points of the amplitude equation (19a) with $v = 0$.

For any given h, Eq. (23) can be regarded as a quadratic equation for the detuning ρ where the coefficients are explicit functions of $|a|^2$. There are two roots $\rho_{1,2}$ for $|a|^2$ smaller than $|a_{\rm res}|^2$, and none for $|a|^2 > |a_{\rm res}|^2$, where $|a_{\rm res}|^2$ is a unique positive root of the equation

$$\frac{64}{\pi^2}|a_{\rm res}|^2\left(\frac{\gamma}{\omega_0} + \frac{\zeta_I}{2}|a_{\rm res}|^2\right)^2 = h^2. \tag{28}$$

The value $|a_{\rm res}|$ defined by Eq. (28) gives the largest amplitude of the wobbling achievable for the given driving strength h. The corresponding value of the detuning,

$$\rho_{\rm res} = \frac{\zeta_R}{2}|a_{\rm res}|^2 < 0, \tag{29}$$

ensures the strongest resonance. As was expected, the strongest resonance is achieved with negative detuning.

C. 1:1 parametrically driven wobbler

For large times, the asymptotic expansion for the damped-driven wobbler is given by Eq. (48) in [18] where we just need to set $v = 0$ and replace ω_0 with Ω,

$$\phi(x,t) = \tanh[(1 - 3|a|^2)\xi] + a\,\mathrm{sech}\xi\tanh\xi\, e^{i\Omega t} + \text{c.c.} + 2|a|^2\mathrm{sech}^2\xi\tanh\xi + a^2 f_1(\xi)\, e^{2i\Omega t} + \text{c.c.} + \mathcal{O}(|a|^3). \tag{30}$$

Here, $\xi = x - x_0$, where x_0 is a constant determined by initial conditions and a is a stable fixed point of the dynamical system (19a) with $v = 0$ [a unique fixed point or one of the two stable fixed points depending on whether h is outside or inside the bistability interval (h_+, h_-)]. The function $f_1(\xi)$ is given by Eq. (12). The interpretation of different terms in Eq. (30) is the same as in the case of the freely wobbling kink [18].

Like the corresponding formula for the free wobbler, expansion (30) is only valid at distances $|\xi|=\mathcal{O}(1)$. For larger distances one has to use the outer expansions

$$\phi = \pm 1 + \epsilon^2\phi_2 + \epsilon^3\phi_3 + \cdots, \tag{31}$$

with coefficients ϕ_n determined as in Sec. V of [18]. The analysis of the outer equations produces results equivalent to those in [18]: the second-harmonic radiation propagates away from the core of the kink at the group velocity, leaving in its wake a sinusoidal wave with the frequency 2Ω, wavenumber $k_0=\sqrt{8}$, and constant amplitude of the order $|a|^2$.

Unlike the case of the free wobbling of the kink, the frequency of the oscillation is not determined by its amplitude but is locked to the frequency of the driver, Ω. Another difference from the undamped-undriven case is that the driven oscillations of the wobbler do not die out as $t\to\infty$. Instead, the amplitude of the oscillations approaches a nonzero constant value, which is determined by the parameters of the damping and the driving and—in the bistable region—by the initial conditions. On the other hand, the asymptotic velocity of the damped-driven wobbler *is* zero.

It is interesting to note that unlike in the case of the parametrically driven damped linear oscillator [19] or damped-driven breather of the sine-Gordon or ϕ^4 equation [20], there is no threshold driving strength in the case of the damped-driven wobbler. No matter how small is h, the amplitude $a(t)$ will not decay to zero as $t\to\infty$.

III. 2:1 PARAMETRIC RESONANCE

A. Asymptotic expansion

It is a textbook fact that the strongest parametric resonance is achieved when the parameter of the oscillator is varied at *double* its natural frequency. With an eye to the detection of the most efficient driving regime for the wobbling kink, we now consider the driving frequency close to twice its natural wobbling frequency,

$$\tfrac{1}{2}\phi_{tt} - \tfrac{1}{2}\phi_{xx} + \gamma\phi_t - [1 + h\cos(2\Omega t)]\phi + \phi^3 = 0. \tag{32}$$

As before,

$$\Omega = \omega_0(1+\rho), \quad \rho = \epsilon^2 R, \quad \gamma = \epsilon^2\Gamma,$$

but now we use a different scaling for h,

$$h = \epsilon^2 H.$$

We transform the equation in exactly the same way as we did in the previous section; this yields

$$\frac{1}{2}(1+\rho)^2\phi_{\tau\tau} - v(1+\rho)\phi_{\xi\tau} - \frac{v_\tau}{2}(1+\rho)\phi_\xi - \frac{1-v^2}{2}\phi_{\xi\xi}$$
$$- \phi + \phi^3 = h\cos(2\omega_0\tau)\phi + \gamma v\phi_\xi - \gamma(1+\rho)\phi_\tau.$$

The perturbation expansion is unchanged from the undamped-undriven case at $\mathcal{O}(\epsilon^1)$. With the addition of the ϵ^2-strong driving, the equation at $\mathcal{O}(\epsilon^2)$ acquires additional terms on the right-hand side as compared to Eq. (7),

$$\frac{1}{2}D_0^2\phi_2 + \mathcal{L}\phi_2 = F_2(X_0, \ldots; T_0, \ldots) + \frac{H}{2}\phi_0\, e^{2i\omega_0 T_0} + \text{c.c.}$$

Here F_2 is as in Eq. (8). The zeroth- and the first-harmonic components of ϕ_2 are not affected by this extra term. Namely, assuming that the solution is of the form (9) and setting $D_1V=0$, we get Eq. (10) for $\varphi_2^{(0)}$ while, imposing $D_1A=0$, Eq. (15) produces $\varphi_2^{(1)}=0$. As for the coefficient function $\varphi_2^{(2)}$, we obtain

$$\varphi_2^{(2)} = A^2 f_1(X_0) + H f_2(X_0), \tag{33}$$

where the function $f_2(X_0)$ satisfies

$$(\mathcal{L} - 6) f_2(X_0) = \tfrac{1}{2}\tanh X_0. \tag{34}$$

We note that the value of 6 lies in the continuous spectrum of the operator $\mathcal{L}$, and so in order to determine $f_2(X_0)$ uniquely, one has to impose two additional conditions fixing the coefficients of two bounded homogeneous solutions that can be added to f_2. We do this by requiring the absence of incoming radiation. The particular solution of Eq. (34) that obeys these radiation boundary conditions is

$$f_2(X_0) = -\tfrac{1}{12} f_1(X_0) + \tfrac{1}{24}\tanh X_0 (2\,\mathrm{sech}^2 X_0 - 3), \tag{35}$$

where the function $f_1(X_0)$ is given by Eq. (12). In what follows, we will use the fact that $f_2(X_0)$ is an odd function.

The first term in the right-hand side of Eq. (33) describes the familiar second-harmonic radiation from the freely wobbling kink. The second term consists of the induced second-harmonic radiation and a standing wave—also excited by the forcing.

At the order ϵ^3, we get Eq. (16) where F_3 is given by Eq. (17) with the term $\frac{1}{2}He^{i\omega_0 T_0}\phi_0$ replaced with $\frac{1}{2}He^{2i\omega_0 T_0}\phi_1$. The amplitude equation for A, which arises as the solvability condition for the first harmonic, is now

$$iD_2A + \frac{\omega_0\zeta}{2}|A|^2A - \omega_0\left(\frac{V^2}{2} + R\right)A = \frac{\omega_0\sigma}{2}HA^* - i\Gamma A, \tag{36}$$

where

$$\sigma = \int_{-\infty}^{\infty}\left[\frac{1}{2}\mathrm{sech}^2 X_0 \tanh^2 X_0 - 6\,\mathrm{sech}^2 X_0 \tanh^3 X_0 f_2(X_0)\right] dX_0.$$

The imaginary part of this integral is

$$\sigma_I = \tfrac{1}{12}\zeta_I = 0.003\,863.$$

For the real part we find, numerically,

$$\sigma_R = 0.5958.$$

The solvability condition for the zeroth harmonic gives

$$D_2V = -2\Gamma V.$$

We finally write the amplitude and the velocity equations in terms of the natural variables $a=\epsilon A$ and $v=\epsilon V$ and the unscaled time t (as in the previous section) as follows:

$$\dot{a} = -\gamma a - i\omega_0 \rho a + \tfrac{1}{2} i\omega_0 \zeta |a|^2 a - \tfrac{1}{2} i\omega_0 v^2 a - \tfrac{1}{2} i\omega_0 \sigma h a^* + \mathcal{O}(|a|^5), \tag{37a}$$

$$\dot{v} = -2\gamma v + \mathcal{O}(|a|^5). \tag{37b}$$

B. Reduced dynamics in two dimensions

As in the previous case of the 1:1 parametrically driven wobbler, the velocity tends to zero as $t \to \infty$ and the evolution of $a(t)$ is governed by the dynamical system (37a) with $v=0$. This two-dimensional dynamical system does not have periodic orbits, as one can readily check using Dulac's criterion. Letting $a=re^{-i\theta}$ and $\sigma=|\sigma|e^{i \operatorname{Arg} \sigma}$, Eq. (37a) yields

$$\dot{r} = -\gamma r + \frac{\omega_0}{2} \zeta_I r [r_0^2 \sin(2\theta + \operatorname{Arg} \sigma) - r^2], \tag{38}$$

where $r_0^2=(|\sigma|/\zeta_I)h$. Since the right-hand side of Eq. (38) is negative for all a with $|a|>r_0$, no trajectories can escape to infinity. Therefore, all trajectories should flow to one of the fixed points. The fixed points are given by the equation

$$\gamma a + i\omega_0 \rho a - i\frac{\omega_0 \zeta}{2} |a|^2 a = -i\frac{\omega_0 \sigma}{2} h a^*. \tag{39}$$

One fixed point is trivial, $a=0$; this fixed point is stable if $h<h_+$, where

$$\frac{|\sigma|^2}{4} h_+^2 = \left(\frac{\gamma}{\omega_0}\right)^2 + \rho^2, \tag{40}$$

and unstable otherwise. For the nontrivial points, we get

$$\mathcal{H}(|a|^2) = h, \tag{41}$$

where

$$\mathcal{H}^2 = \frac{4}{|\sigma|^2}\left[\left(\frac{\gamma}{\omega_0} + \frac{\zeta_I}{2}|a|^2\right)^2 + \left(\rho - \frac{\zeta_R}{2}|a|^2\right)^2\right].$$

Assume, first, that $\rho>\rho_0$, where

$$\rho_0(\gamma) = \frac{1}{\omega_0}\frac{\zeta_I}{\zeta_R}\gamma = -0.03146\gamma. \tag{42}$$

The function $\mathcal{H}(|a|^2)$ with ρ in this parameter range is monotonically growing, from h_+ to infinity. Equation (41) has one root provided $h>h_+$, and no roots otherwise. Consequently, in the region $h>h_+$ the dynamical system (37) has two stable fixed points a_1 and $-a_1$, where

$$|a_1|^2 = \frac{2\alpha + \sqrt{|\zeta\sigma|^2 h^2 - 4\beta^2}}{|\zeta|^2}, \tag{43}$$

with α and β as in Eq. (26b). In the region $h<h_+$, the (stable) fixed point at the origin is the only fixed point available in the system. (Thus we have a supercritical pitchfork bifurcation as h is increased through $h=h_+$.)

Assume now $\rho<\rho_0$. As $|a|^2$ grows from zero to infinity, the function $\mathcal{H}$ decreases from h_+ to its lowest value of h_-, where

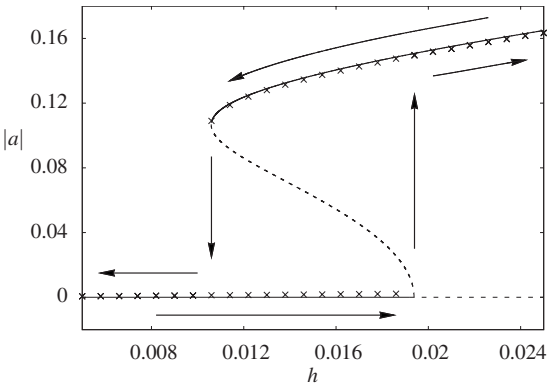

FIG. 2. The hysteresis loop in the 2:1 parametrically driven ϕ^4 equation [Eq. (32)] with $\gamma=0.005$ and $\rho=-0.005$. The driving strength is increased from 0.005 to 0.025 in increments of 8×10^{-4} and then reduced back to 0.005. Crosses mark results of simulations of Eq. (32). The continuous and the dashed lines show the stable and the unstable fixed points of the amplitude equation (37a) with $v=0$.

$$\frac{|\sigma|^2}{4} h_-^2 = \frac{1}{|\zeta|^2}\left(\zeta_R \frac{\gamma}{\omega_0} + \zeta_I \rho\right)^2, \tag{44}$$

and then increases to infinity. Therefore, for $\rho<\rho_0$, the dynamical system (37) has one fixed point at the origin for small driving strengths $0<h<h_-$; five fixed points a_1, a_2, 0, $-a_1$, and $-a_2$ for the intermediate strengths $h_-<h<h_+$; and three fixed points a_1, 0, and $-a_1$ for $h>h_+$. Here h_+ is given by Eq. (40) and h_- is given by Eq. (44). The nontrivial fixed points a_1 and a_2 are born in a saddle-node bifurcation at $h=h_-$. At $h=h_+$, a subcritical pitchfork bifurcation occurs; here, the point a_2 merges with the trivial fixed point. Therefore, out of the two nontrivial fixed points a_1 and a_2, the stable one is a_1, i.e., the fixed point with the larger absolute value—given by Eq. (43). In summary, for $h<h_-$ all trajectories flow to the origin; for $h>h_+$, they are attracted to the nontrivial fixed points $\pm a_1$; and, finally, in the region $h_-<h<h_+$, we have a tristability between $a=0$ and $a=\pm a_1$.

These predictions of the amplitude equation were compared to results of direct numerical simulations of Eq. (32), with $\gamma=0.005$. As in the previous section, we increased h, past h_+, and then reduced it to values under h_-. Figure 2 shows the hysteresis loop arising for $\rho=-0.005$. For $\rho=-0.003$ the hysteresis was less pronounced and for $\rho=0$ it was seen to disappear completely. These observations are consistent with the value of the critical detuning (42) which, for $\gamma=0.005$, equals $\rho_0=-1.573\times10^{-4}$. The bifurcation values $h_\pm$ observed in simulations with $\rho=-0.005$ ($h_+=0.019$ and $h_-=0.011$) are also in agreement with the predictions of the amplitude equation (which gives $h_+=0.01938$ and $h_-=0.01059$).

C. 2:1 parametrically driven wobbler

Restricting ourselves to the $t\to\infty$ asymptotic behavior of $\phi(x,t)$, the leading orders of the perturbation expansion in the case of the subharmonic response are

$$\phi(x,t) = \tanh[(1-3|a|^2)\xi] + a\ \mathrm{sech}\xi\ \tanh\xi\ e^{i\Omega t} + \text{c.c.} + 2|a|^2\mathrm{sech}^2\,\xi\ \tanh\xi + [a^2 f_1(\xi) + h f_2(\xi)]e^{2i\Omega t} + \text{c.c.} + \mathcal{O}(|a|^3). \quad (45)$$

Here, $\xi = x - x_0$; a is a stable fixed point (zero or nonzero) given by one of the roots of Eq. (39); and the functions f_1 and f_2 are defined by Eqs. (12) and (35), respectively. The main difference from the case of the 1:1 parametric resonance is that the amplitude of the wobbling approaches a nonzero value only if the driver's strength exceeds a certain threshold; this threshold value is given by h_+ in the region $\rho > \rho_0$ and by h_- in the region $\rho < \rho_0$. If h lies below the threshold, the wobbling dies out and we need to set $a=0$ in Eq. (45). We also note that the 2:1 resonant driving excites a standing wave and radiation with the frequency 2Ω and an amplitude proportional to h [the f_2 term in Eq. (45)].

Like Eq. (30) of the previous section, expansion (45) is only valid on the length scale $\xi = \mathcal{O}(1)$. To describe the waveform at longer distances, we need to invoke the outer expansions (31). Evaluating the coefficient of the term ϵ^2 in these expansions and matching it to the "inner" expression (33) in the overlap region, we obtain

$$\phi_2 = \pm \mathcal{J} B_\pm\, e^{i(2\omega_0 T_0 \mp k_0 X_0)} + \text{c.c.} - \frac{H}{4}\cos(2\omega_0 T_0), \quad (46)$$

where the top and the bottom signs pertain to the regions $X_0 > 0$ and $X_0 < 0$, respectively. In Eq. (46), $\mathcal{J} = (2 - ik_0)J_2^\infty$ and the functions $B_\pm = B_\pm(X_1, X_2, \ldots; T_1, T_2, \ldots)$ satisfy

$$B_\pm(0,0,\ldots;T_1,T_2,\ldots) = A^2(0,0,\ldots;T_2,T_3,\ldots) - \frac{H}{96}. \quad (47)$$

Equation (47) represents the boundary condition for the amplitudes $B_\pm$; the equations of motion for these variables arise at the order ϵ^3 and coincide with Eqs. (33) of [18]. The solution of these equations with the boundary condition (47) is qualitatively similar to the solution with the "undriven" boundary condition $B_\pm(0,0,\ldots;T_1,T_2,\ldots) = A^2(0,0,\ldots;T_2,T_3,\ldots)$. Namely, we have two outward-propagating waves leaving the amplitudes $B_\pm$ equal to the constant $A^2 - H/96$ in their wake.

IV. HARMONIC VERSUS SUBHARMONIC PARAMETRIC RESONANCE: QUALITATIVE COMPARISON

With the amount of detail that we had to provide to justify our conclusions and derivations, the resonance mechanisms of the driven wobbling kink may not be easy to crystallize. The purpose of this short section is to discuss the two parametric resonances qualitatively—in particular, to comment on their atypical hierarchy.

We observed that the amplitude $|a|$ is of order $h^{1/3}$ in the case of the harmonic resonance (i.e., the resonance arising when the driving frequency ω_d is near ω_0) but only $\mathcal{O}(h^{1/2})$ in the case of the subharmonic resonance (the resonance arising for $\omega_d \approx 2\omega_0$). Thus the harmonic resonance is stronger than the subharmonic one, and this is precisely the opposite behavior to what we might naively expect based on our intuition about the parametric driving.

To explain this surprising behavior qualitatively, we write the term $h\cos(n\Omega t)\phi$ in Eqs. (1) and (32) as $h\cos(n\Omega t)\phi_0$ plus terms of order ha and smaller. This representation reveals that what was introduced as a parametric driver is, to the leading order, an external (direct) driving force. This driving force is nonhomogeneous, i.e., its magnitude and direction vary with the distance, and it has odd spatial parity. When $n=1$, the frequency of this driving force coincides with the natural frequency of the wobbler and its spatial parity coincides with the parity of the wobbling mode (which is also odd). As a result, we have a strong direct resonance.

When $n=2$, the external force $h\cos(2\Omega t)\phi_0$ is not in resonance with the wobbling frequency. However the function $h\cos(2\Omega t)$ acts as a parametric driver on the *next* term in the expansion of ϕ — that is, the product $h\cos(2\Omega t)\epsilon\phi_1$ has a component with the resonant frequency. Importantly, this term has the "correct" odd parity as a function of ξ.

In addition, the odd-parity force $h\cos(2\Omega t)\phi_0$ generates odd-parity radiation and the odd-parity standing wave, both with the frequency 2Ω. This radiation and standing wave also couple to the wobbling mode, via the term $\epsilon^3\phi_0\phi_1\phi_2$ in Eq. (32). This constitutes a concurrent driving mechanism. Since each of the two mechanisms is indirect (i.e., requires the wobbling mode as a mediator for the frequency halving) and since the resulting effective driving strength is proportional to the amplitude of the wobbling mode (assumed small), the response to the frequency 2Ω is weaker than to Ω.

V. 1:2 DIRECT RESONANCE

A. Perturbation expansion

We start with the direct driving at *half* the natural wobbling frequency. This and the following case of the 1:1 direct resonance were previously considered by Quintero *et al.* [2,3] and so we will be able to compare our results to theirs. The equation is

$$\frac{1}{2}\phi_{tt} - \frac{1}{2}\phi_{xx} + \gamma\phi_t - \phi + \phi^3 = h\cos\left(\frac{\Omega}{2}t\right), \quad (48)$$

where, as in the previous sections, $\Omega = \omega_0(1+\rho)$. As before, we change the time variable, so that $\Omega t = \omega_0 \tau$ and transform the equation to the moving frame,

$$\frac{1}{2}(1+\rho)^2\phi_{\tau\tau} - v(1+\rho)\phi_{\xi\tau} - \frac{v_\tau}{2}(1+\rho)\phi_\xi - \frac{1-v^2}{2}\phi_{\xi\xi} - \phi + \phi^3 = h\cos\left(\frac{\omega_0}{2}\tau\right) + v\gamma\phi_\xi - \gamma(1+\rho)\phi_\tau. \quad (49)$$

Keeping our standard scalings for the small parameters γ and ρ,

$$\gamma = \epsilon^2\Gamma, \quad \rho = \epsilon^2 R,$$

we choose a fractional-power scaling law for h,

$$h = \epsilon^{3/2}H.$$

This scaling will be shown to produce a balance of damping and driving terms at the leading order in the amplitude equation. Expanding ϕ in powers of $\epsilon^{1/2}$,

$$\phi = \phi_0 + \epsilon\phi_1 + \epsilon^{3/2}\phi_{3/2} + \epsilon^2\phi_2 + \epsilon^{5/2}\phi_{5/2} + \cdots,$$

where $\phi_0 = \tanh X_0$, and substituting in Eq. (49) we obtain Eq. (6) for ϕ_1. The partial differential equation arising at $\mathcal{O}(\epsilon^{3/2})$ is

$$\frac{1}{2}D_0^2\phi_{3/2} + \mathcal{L}\phi_{3/2} = \frac{H}{2}e^{i(\omega_0/2)T_0} + \text{c.c.}$$

Discarding the homogeneous solutions, the solution $\phi_{3/2}$ to this equation can be chosen in the form $\phi_{3/2} = \varphi_{3/2}^{(1/2)}e^{i(\omega_0/2)T_0} + \text{c.c.}$, where the coefficient function $\varphi_{3/2}^{(1/2)}$ satisfies the linear nonhomogeneous equation

$$\left(\mathcal{L} - \frac{3}{8}\right)\varphi_{3/2}^{(1/2)} = \frac{H}{2}.$$

Since $\frac{3}{8}$ is not an eigenvalue of the operator $\mathcal{L}$, this equation has a unique bounded solution. To determine it, we note that two homogeneous solutions of this equation, i.e., solutions of $(\mathcal{L} - 3/8)y = 0$, are given by Segur's formula

$$y_p(X_0) = \frac{1}{(1+ip)(2+ip)}e^{ipX_0} \times (2 - p^2 - 3ip\tanh X_0 - 3\,\text{sech}^2 X_0) \quad (50)$$

with $p = \pm i\sqrt{13/4}$ [21]. Using these in the variation of parameters, we obtain

$$\varphi_{3/2}^{(1/2)} = \tfrac{4}{13}H(1 - 8\,\text{sech}^2 X_0).$$

The term $\varphi_{3/2}^{(1/2)}e^{i(\omega_0/2)T_0}$ in the expansion of the wobbling kink represents the background stationary wave induced by the driver.

The equations arising at $\mathcal{O}(\epsilon^2)$ are the same as for the free wobbler and the 1:1 parametric resonance [Eqs. (7) and (8)]. Hence the coefficients of the harmonic components of ϕ_2 are the same as in the undamped-undriven case. Namely, imposing the solvability conditions $D_1V = 0$ and $D_1A = 0$, we obtain Eq. (10) for $\varphi_2^{(0)}$ and Eq. (11) for $\varphi_2^{(2)}$. We also impose Eq. (15) to obtain $\varphi_2^{(1)} = 0$.

At the order $\epsilon^{5/2}$ we have the equation

$$\tfrac{1}{2}D_0^2\phi_{5/2} + \mathcal{L}\phi_{5/2} = -6\phi_0\phi_1\phi_{3/2} + VD_0\partial_0\phi_{3/2}.$$

Its solution consists of the $\frac{1}{2}$th and the $\frac{3}{2}$th harmonics with the coefficient functions

$$\varphi_{5/2}^{(1/2)} = HAu_a(X_0) + i\omega_0 HVu_b(X_0),$$

$$\varphi_{5/2}^{(3/2)} = HAu_c(X_0),$$

respectively. Here the functions u_a, u_b, and u_c satisfy

$$\left(\mathcal{L} - \tfrac{3}{8}\right)u_a(X_0) = -\tfrac{24}{13}(1 - 8\,\text{sech}^2 X_0)\text{sech}\,X_0\tanh^2 X_0,$$

$$\left(\mathcal{L} - \tfrac{3}{8}\right)u_b(X_0) = \tfrac{32}{13}\text{sech}^2 X_0\tanh X_0,$$

and

$$\left(\mathcal{L} - \tfrac{27}{8}\right)u_c(X_0) = -\tfrac{24}{13}(1 - 8\,\text{sech}^2 X_0)\,\text{sech}\,X_0\tanh^2 X_0.$$

In order to determine $u_c(X_0)$ uniquely, we impose the radiation boundary conditions. (These are necessary because the value $\frac{27}{8}$ lies in the continuous spectrum of the operator $\mathcal{L}$.) The functions u_a and u_c are even, while u_b is odd. These three functions can be easily found by solving the above nonhomogeneous boundary-value problems numerically.

Proceeding to the order ϵ^3, we find Eq. (16), where F_3 is given by Eq. (17) with the term $\frac{1}{2}He^{i\omega_0T_0}\phi_0 + \text{c.c.}$ replaced with $-3\phi_0\phi_{3/2}^2$. The solvability conditions for this equation are

$$D_2V = -2\Gamma V \quad (51)$$

for the zeroth harmonic, and

$$D_2A = -\Gamma A - i\omega_0 RA + \tfrac{i}{2}\zeta\omega_0|A|^2A - \tfrac{i}{2}\omega_0V^2A + \tfrac{60}{169}i\omega_0\pi H^2 \quad (52)$$

for the first harmonic. The latter equation includes both the damping and the driving terms and so the resulting master equations could be expected to capture the essentials of the nearly stationary wobbling of the kink (i.e., wobbling in the vicinity of the fixed point of the amplitude equations, which arises due the balance of the damping and the driving terms). However the description provided by these amplitude equations — while being qualitatively correct — turns out to be insufficiently accurate when compared to numerical simulations of the full partial differential equation (48). (The source of this inaccuracy will be clarified below.) In search of greater accuracy, we shall proceed to higher orders.

The solution of Eq. (16) has the form

$$\phi_3 = \varphi_3^{(0)} + \varphi_3^{(1)}e^{i\omega_0T_0} + \text{c.c.} + \varphi_3^{(2)}e^{2i\omega_0T_0} + \text{c.c.} + \varphi_3^{(3)}e^{3i\omega_0T_0} + \text{c.c.}$$

The function $\varphi_3^{(2)}$ is calculated to be zero; the coefficient of the zeroth harmonic is given by

$$\varphi_3^{(0)} = \tfrac{16}{169}H^2(45X_0\,\text{sech}^2 X_0 - 3\tanh X_0 - 128\,\text{sech}^2 X_0\tanh X_0),$$

and the one for the first-harmonic component is

$$\varphi_3^{(1)} = -\partial_2 AX_0\,\text{sech}\,X_0\tanh X_0 + |A|^2Au_d(X_0) - \tfrac{2}{3}i\omega_0(\Gamma + i\omega_0R)(3 - 4\,\text{sech}^2 X_0) + H^2u_e(X_0), \quad (53)$$

where the functions $u_d(X_0)$ and $u_e(X_0)$ are the bounded solutions of the following nonhomogeneous equations:

$$\left(\mathcal{L} - \tfrac{3}{2}\right)u_d = \tfrac{3}{2}\zeta\,\text{sech}\,X_0\tanh X_0 + 6\,\text{sech}\,X_0\tanh^2 X_0\left[3X_0\,\text{sech}^2 X_0 - \tfrac{5}{2}\text{sech}^2 X_0\tanh X_0 - f_1(X_0)\right],$$

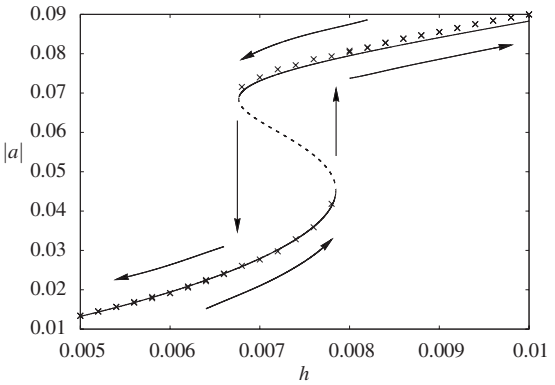

FIG. 3. The hysteresis loop in the 1:2 directly driven ϕ^4 equation [Eq. (48)] with $\gamma=0.001$ and $\rho=-0.002$. The driving strength h is increased from 0.005 to 0.01 in increments of 0.0002 and then reduced back to 0.005 (as indicated by the arrows). Crosses mark results of simulation of the partial differential equation [Eq. (48)]. The continuous and the dashed lines depict the stable and the unstable fixed points of the amplitude equation (58a) with $v=0$.

$$\left(\mathcal{L}-\tfrac{3}{2}\right)u_e = -\tfrac{48}{169}H^2 \tanh X_0 (1-8\ \mathrm{sech}^2 X_0)^2 + \tfrac{180}{169}\pi\ \mathrm{sech}\ X_0 \tanh X_0. \tag{54}$$

Since $(\mathcal{L}-3/2)$ is a parity-preserving operator while the right-hand sides of the above equations are given by odd functions, and since the homogeneous solution $y_w = \mathrm{sech}\ X_0 \tanh X_0$ is also an odd function, it follows that the nonhomogeneous solutions u_d and u_e are both odd. This is the only fact about u_d and u_e that we will need in this section—we do not need to know any details of these functions here. Nevertheless, we do evaluate the solution u_d as it will be required later on, in the study of the 1:1 directly driven kink (Sec. VI); we evaluate it using the variation of parameters and numerical integration. The nonhomogeneous solution is defined up to the addition of an arbitrary multiple of y_w; however, this extra degree of freedom is fictitious as it can always be eliminated by a suitable rescaling of ϵ. [Accordingly, the extra term proportional to y_w cancels in the integral η where it appears in Sec. VI and does not contribute to the amplitude equations (75).]

To eliminate the quasisecular term proportional to $X_0\ \mathrm{sech}\ X_0 \tanh X_0$ in Eq. (53), we set $\partial_2 A=0$.

It will not be necessary to calculate the third-harmonic component $\varphi_3^{(3)}$ as this does not contribute to the zeroth or the first harmonics at $\mathcal{O}(\epsilon^4)$, and hence does not affect the ϵ^4 correction to the amplitude equations. Similarly, we shall not calculate $\phi_{7/2}$ as it only contains fractional harmonic components, which cannot impinge on the amplitude equations at $\mathcal{O}(\epsilon^4)$. Hence we skip the order $\epsilon^{7/2}$.

At $\mathcal{O}(\epsilon^4)$, we obtain

$$\tfrac{1}{2}D_0^2\phi_4 + \mathcal{L}\phi_4 = F_4, \tag{55}$$

where

$$\begin{aligned} F_4 = {} & (\partial_0\partial_1 - D_0D_1)\phi_3 + (\partial_0\partial_2 - D_0D_2)\phi_2 + \tfrac{1}{2}(\partial_1^2 - D_1^2)\phi_2 \\ & + (\partial_0\partial_3 - D_0D_3)\phi_1 + (\partial_1\partial_2 - D_1D_2)\phi_1 - 3\phi_1^2\phi_2 \\ & - 6\phi_0\phi_1\phi_3 - 6\phi_0\phi_{3/2}\phi_{5/2} - 3\phi_0\phi_2^2 + VD_0\partial_0\phi_3 \\ & + VD_0\partial_1\phi_2 + VD_0\partial_2\phi_1 + VD_1\partial_0\phi_2 + VD_1\partial_1\phi_1 \\ & + VD_2\partial_0\phi_1 + \tfrac{1}{2}D_2V\partial_0\phi_1 + \tfrac{1}{2}D_3V\partial_0\phi_0 - \tfrac{1}{2}V^2\partial_0^2\phi_2 \\ & - V^2\partial_0\partial_1\phi_1 - \Gamma D_0\phi_2 - \Gamma D_1\phi_1 + \Gamma V\partial_0\phi_1 - RD_0^2\phi_2 \\ & + VRD_0\partial_0\phi_1. \end{aligned}$$

The corresponding solvability conditions are

$$D_3V = 0 \tag{56}$$

and

$$D_3A = -\tfrac{1}{2}i\omega_0\lambda H^2 A, \tag{57}$$

where

$$\begin{aligned} \lambda = \int_{-\infty}^{\infty} \mathrm{sech}\ X_0 \tanh X_0 \Bigg[& -\frac{96}{169}(45X_0\ \mathrm{sech}^2 X_0 - 3\tanh X_0 \\ & - 128\ \mathrm{sech}^2 X_0 \tanh X_0)\mathrm{sech}\ X_0 \tanh^2 X_0 \\ & - \frac{24}{13}\tanh X_0 (1-8\ \mathrm{sech}^2 X_0)u_a(X_0) \\ & - \frac{24}{13}\tanh X_0\ (1-8\ \mathrm{sech}^2 X_0)u_c(X_0) \\ & - \frac{96}{169}\mathrm{sech}\ X_0 \tanh X_0\ (1-8\ \mathrm{sech}^2 X_0)^2 \Bigg] dX_0. \end{aligned}$$

Numerically,

$$\lambda = \lambda_R + i\lambda_I = -7.4656 - i1.6785.$$

Expanding the derivative $\partial/\partial\tau$ as $D_0+\epsilon D_1+\epsilon^2 D_2+\cdots$ and recalling that $d\tau/dt=1+\rho$, we combine Eqs. (52) and (57). We also combine Eqs. (51) and (56). This yields a system of two master equations:

$$\begin{aligned} \dot{a} = {} & -\gamma a - i\omega_0\rho\, a + i\frac{\omega_0\zeta}{2}|a|^2 a - i\frac{\omega_0}{2}v^2 a \\ & + i\frac{60}{169}\pi\omega_0\, h^2 - \frac{1}{2}i\omega_0\,\lambda h^2 a + \mathcal{O}(|a|^5), \end{aligned} \tag{58a}$$

$$\dot{v} = -2\gamma v + \mathcal{O}(|a|^5). \tag{58b}$$

It is essential to combine the slow-scale equations in this way, rather than solving the individual equations with the assumption that the different scales are independent. Solving individual equations separately would be illegitimate because in integrating the equations one is covering more than one time scale. For example, solving Eqs. (56) and (57) we would be integrating over the scale T_3, which includes a shorter time scale T_2.

All terms in the right-hand side of Eq. (58a) are of order $|a|^3$, except the last term which is $\mathcal{O}(|a|^4)$. This last term is the correction coming from the fourth order of the perturbation expansion. As we have already mentioned, the ampli-

tude equations (58) without this term produce an inaccurate description of the dynamics in the region of interest (i.e., in the vicinity of the fixed points). On the other hand, if the above fourth-order term is included, the predictions of the amplitude equations (58) turn out to be in good agreement with results of the direct numerical simulations of the full partial differential equation (48) (see Fig. 3). The substantial improvement in accuracy is due to the large value of the coefficient λ.

B. Reduced two-dimensional system

Introducing the notation

$$\gamma' = \gamma - \frac{\lambda_I}{2}\omega_0 h^2, \quad \rho' = \rho + \frac{\lambda_R}{2}h^2, \quad h' = -\frac{480}{169}h^2,$$

the amplitude equation (58a) can be written as

$$\dot{a} = -\gamma' a - i\omega_0 \rho' a + i\frac{\zeta}{2}\omega_0 |a|^2 a - \frac{i}{2}\omega_0 v^2 a - i\frac{\pi}{8}\omega_0 h' + \mathcal{O}(|a|^5), \tag{59}$$

which has the same form as the amplitude equation for the 1:1 parametric resonance (19a). Consequently, the dynamics of the 1:2 directly driven wobbling kink will have some similarities with the dynamics of the wobbler driven by the 1:1 parametric force.

According to Eq. (58b), the velocity will be damped until it is so small $[\mathcal{O}(|a|^3)]$ that it can be disregarded in Eq. (58a); hence, after an initial transient the dynamics will be governed by Eq. (58a) with $v=0$. Similarly to Eq. (19) with $v=0$, Eq. (58a) does not have closed orbits. All trajectories crossing the circle $|a|=\frac{60}{169}\pi\omega_0 h^2/\gamma$ flow inward and so no trajectories can escape to infinity. Therefore, all trajectories must flow toward fixed points. If a is a fixed point, the absolute value $|a|$ satisfies

$$h^4\left[\frac{1}{4}|\lambda|^2 - \frac{\pi^2}{|a|^2}\left(\frac{60}{169}\right)^2\right] + h^2\left[\lambda_R\left(\rho - \frac{1}{2}\zeta_R|a|^2\right) - \lambda_I\left(\frac{\gamma}{\omega_0} + \frac{1}{2}\zeta_I|a|^2\right)\right] + \left(\rho - \frac{1}{2}\zeta_R|a|^2\right)^2 + \left(\frac{\gamma}{\omega_0} + \frac{1}{2}\zeta_I|a|^2\right)^2 = 0. \tag{60}$$

The left-hand side of this equation is a biquadratic in h. Solving for h we obtain an explicit expression for $h=h_{1,2}(|a|^2)$; the roots $|a|^2$ are found by inverting these explicit functions for each ρ, γ, and h. The lower branch of the biquadratic is plotted in Fig. 3 along with results from the numerical simulations of the full partial differential equation (48). We note that, as in the 1:1 parametrically driven ϕ^4 equation, there is no threshold driving strength for the existence of the nonzero wobbling amplitude here.

Here it is appropriate to recall that ρ and γ were assumed to be of the same order while h is $\mathcal{O}(\gamma^{3/4})$. As in the case of system (19a), the absence or the presence of hysteresis in the dynamics depends on whether ρ is above or below the critical value $\rho_0(\gamma)$ given by Eq. (25). If the difference $\rho-\rho_0$ is positive and of order γ, there is only one root $|a|$ for each value of h. The corresponding fixed point is obviously stable. If, on the other hand, the difference $\rho-\rho_0$ is negative (but still of order γ), we have three roots $|a|^2$ for each $h=\mathcal{O}(\gamma^{3/4})$ in the interval (h_+,h_-). These roots correspond to three fixed points, two of which are stable (see Fig. 3). The values h_+ and h_- at which the subcritical bifurcations occur, are given, approximately, by

$$h_\pm^2 = \frac{1}{\mathfrak{c}_0}(P_\pm + \sqrt{P_\pm^2 + 2\mathfrak{c}_0 Q_\pm}), \tag{61}$$

where

$$P_\pm = \frac{1}{18}[\mathfrak{c}_1(3\beta^2 - 5\alpha^2) + 6\alpha\delta \mp (4\mathfrak{c}_1\alpha - 3\delta)\sqrt{\alpha^2 - 3\beta^2}],$$

$$Q_\pm = \frac{1}{27}[\alpha(\alpha^2 + 9\beta^2) \mp (\alpha^2 - 3\beta^2)^{3/2}],$$

$$\mathfrak{c}_0 = 2\left(\frac{30\pi}{169}\right)^2 |\zeta|^4 = 0.3280,$$

$$\mathfrak{c}_1 = \zeta_R\lambda_R + \zeta_I\lambda_I = 6.2747,$$

$$\delta = |\zeta|^2\left(\lambda_R\rho - \lambda_I\frac{\gamma}{\omega_0}\right),$$

and α and β are defined by Eq. (26b). For $\gamma=10^{-3}$ and $\rho=-2\times10^{-3}$, the bifurcation values obtained from Eq. (61) are $h_+=6.74\times10^{-3}$ and $h_-=7.78\times10^{-3}$ while the numerical simulations of the full partial differential equation give $6.6\times10^{-3}<h_+<6.8\times10^{-3}$ and $7.8\times10^{-3}<h_-<8.0\times10^{-3}$. For $\rho=-3\times10^{-3}$, the simulations show a more pronounced hysteresis loop, whereas for $\rho=-1\times10^{-3}$ the hysteresis was seen to disappear. (In both cases γ was kept at 10^{-3}.) These observations are consistent with the value of ρ_0 given by the amplitude equations. [For $\gamma=10^{-3}$, Eq. (25) gives $\rho_0=-1.1\times10^{-3}$.]

C. 1:2 directly driven wobbler

Finally, we produce the first several orders of the perturbation expansion for the 1:2 directly driven wobbling kink. We have

$$\phi(x,t) = \tanh[(1-3|a|^2)\xi] + a\,\mathrm{sech}\xi\tanh\xi e^{i\Omega t} + \mathrm{c.c.} + \tfrac{4}{13}h(1-8\,\mathrm{sech}^2\xi)\,e^{i(\Omega/2)t} + \mathrm{c.c.} + 2|a|^2\mathrm{sech}^2\,\xi\tanh\,\xi + a^2 f_1(\xi)\,e^{2i\Omega t} + \mathrm{c.c.} + \mathcal{O}(|a|^{5/2}). \tag{62}$$

When t is sufficiently large, the variable ξ in this expression equals $x-x_0$ (where x_0 is a constant determined by the initial conditions) and a is a stable fixed point of system (58a) with $v=0$ [a unique fixed point or one of the two stable fixed points depending on whether h is outside or inside the bistability interval (h_+,h_-).]

The interpretation of terms in Eq. (62) is the same as in the previous sections. The frequency of the wobbling [where the wobbling mode is given by the sum of the third and the second terms in the first line in Eq. (62)] is locked to double the driving frequency. The term proportional to h in the second line describes a standing wave induced by the driver. As in the previous sections, expansion (62) is only valid at the length scale $|\xi|=\mathcal{O}(1)$. The standard analysis involving outer expansions demonstrates that, for larger distances, we have groups of second-harmonic radiation waves moving away from the kink and leaving in their wake a sinusoidal waveform of constant amplitude.

D. Qualitative analysis

The driving term $h\cos(\frac{\Omega}{2}t)$ is not in resonance with the natural frequency of the wobbler nor does its parity coincide with the parity of the wobbling mode. Therefore the ability of the 1:2 direct driving to sustain the wobbling is surprising and requires a qualitative explanation.

The authors of [2] proposed that the mechanism which brings about the unexpected superharmonic resonance is the coupling of the translation and the wobbling modes. Our explanation for this phenomenon is rather different and unrelated to the translation mode. The way the driver affects the wobbler is by exciting an even-parity standing wave ($\phi_{3/2}$) at the frequency $\Omega/2$ which then undergoes nonlinear frequency doubling and parity transmutation through the term $\epsilon^3\phi_0\phi_{3/2}^2$ in Eq. (48). This latter term serves as an effective driver to the wobbling mode; it has the resonant frequency and the "correct" parity.

Since this mechanism involves a two-stage process and the resulting effective driving strength is proportional to h^2, this type of driving produces a relatively weak response.

E. Chaotic wobblers?

The authors of Refs. [2,3] observed chaotic kink dynamics in numerical simulations of the 1:2 directly driven wobbling kink. An indirect confirmation of the existence of chaotic motions comes also from the collective-coordinate approach which predicts an unbounded growth of the kink's width, energy, and velocity at resonance [2,3]. On the other hand, our amplitude equations (58) with $\gamma\neq 0$ reduce to a two-dimensional dynamical system, which can obviously not exhibit any chaotic attractors.

To find an explanation for this disagreement, we have carried out a series of numerical simulations of the partial differential equation (48) at a range of driving strengths and damping coefficients. In all our experiments, we confined ourselves to zero detuning, $\rho=0$. We could not detect any sign of chaotic dynamics for h smaller than a certain minimum value, not even in the undamped case. However for h greater or equal than 0.05 and sufficiently small γ, our numerical simulations did reveal kinks performing erratic motion, where initially close profiles were seen to diverge exponentially fast. For $h=0.05$, 0.06, and 0.08, chaos was observed in simulations with γ smaller or equal to 10^{-3}, 2×10^{-3}, and 6×10^{-3}, respectively, whereas the same sequence of h values paired with $\gamma=2\times10^{-3}$, 3×10^{-3}, and 7×10^{-3}, respectively, did not feature any chaotic trajectories. Therefore chaotic attractors may only arise when the damping is extremely weak, much weaker than $\mathcal{O}(h^{4/3})$. This could be the reason why the chaotic dynamics is not captured by our amplitude equations (58) which have been derived on the assumption that $h=\mathcal{O}(\epsilon^{3/2})$ and $\gamma=\mathcal{O}(\epsilon^2)$.

The description of chaotic motions by means of amplitude equations is a topic of future research. We plan to verify whether our asymptotic method will remain applicable in this situation, with the appropriate adjustment of the scaling laws of the variables a and v parameters of the damping and driving.

VI. 1:1 DIRECT RESONANCE

A. Multiscale expansion

Finally, we explore the effect of the direct driving near the natural wobbling frequency of the kink. The equation is

$$\tfrac{1}{2}\phi_{tt}-\tfrac{1}{2}\phi_{xx}+\gamma\phi_t-\phi+\phi^3=h\cos(\Omega t), \tag{63}$$

where $\Omega=\omega_0(1+\rho)$. We let $a=\epsilon A$ and adopt the following scalings for the three small parameters:

$$h=\epsilon H,\quad \gamma=\epsilon^2\Gamma,\quad \rho=\epsilon^2 R. \tag{64}$$

This time, we assume that the velocity is scaled as $v=\epsilon^2 V$ (and not as $v=\epsilon V$). We shall find a nontrivial evolution equation for v, and with the above scalings, the leading-order dynamics of a and v will occur on the same time scale. While other scalings could be investigated, the variables v and a would then change on different time scales and so would effectively be decoupled for small ϵ. Therefore, the chosen scalings correspond to the richest, three-dimensional, dynamics. Rescaling the time so that $\Omega t=\omega_0\tau$ and transforming to the moving frame as in Eq. (4), Eq. (63) becomes

$$\frac{1}{2}(1+\rho)^2\phi_{\tau\tau}-v(1+\rho)\phi_{\xi\tau}-\frac{v_\tau}{2}(1+\rho)\phi_\xi-\frac{1-v^2}{2}\phi_{\xi\xi}-\phi+\phi^3=h\cos(\omega_0\tau)+v\gamma\phi_\xi-\gamma(1+\rho)\phi_\tau. \tag{65}$$

We expand ϕ as in Eq. (5).

With the driving amplitude of the order ϵ, the linear perturbation consists of the wobbling mode and a standing wave excited by the driver,

$$\phi_1 = [A \text{ sech } X_0 \tanh X_0 + H(1 - 2 \text{ sech}^2 X_0)]\, e^{i\omega_0 T_0} + \text{c.c.}$$

Next, at $\mathcal{O}(\epsilon^2)$, we obtain Eq. (7) with

$$F_2 = (\partial_0\partial_1 - D_0 D_1)\phi_1 - 3\phi_0\phi_1^2.$$

Discarding solutions to the corresponding homogeneous equation, the solution to Eq. (7) will consist only of the harmonics present in the forcing, i.e., it will have the form (9). The solvability condition for the first-harmonic component is $D_1 A = 0$; assuming that this condition is in place, we obtain $\varphi_2^{(1)}(X_0) = -\partial_1 A X_0 \text{ sech } X_0 \tanh X_0$. To avoid the quasisecular behavior at infinity we impose $\partial_1 A = 0$, which results in

$$\varphi_2^{(1)} = 0. \tag{66}$$

The other two harmonic components of the quadratic correction ϕ_2 have the coefficients

$$\begin{aligned}\varphi_2^{(0)} = {} & |A|^2 \text{sech}^2 X_0 (2 \tanh X_0 - 3X_0) \\ & + H^2(9X_0 \text{ sech}^2 X_0 - 3 \tanh X_0 - 8 \text{ sech}^2 X_0 \tanh X_0) \\ & - 4H(A + A^*) \text{ sech } X_0 (1 + \text{sech}^2 X_0)\end{aligned} \tag{67}$$

and

$$\varphi_2^{(2)} = A^2 f_1(X_0) + AH f_3(X_0) + H^2 f_4(X_0), \tag{68}$$

where f_1 is as in Eq. (12), and the functions f_3 and f_4 are defined by

$$\begin{aligned}f_3(X_0) = {} & \tfrac{1}{2}\text{sech } X_0 - 4 \text{ sech}^3 X_0 - \tfrac{15}{32} i k_0 \\ & \times (3 - \tanh^2 X_0 + i k_0 \tanh X_0) \\ & \times [J_1^*(X_0) - J_1^\infty]\, e^{i k_0 X_0} \\ & + \tfrac{15}{32} i k_0 (3 - \tanh^2 X_0 - i k_0 \tanh X_0)\, J_1(X_0)\, e^{-i k_0 X_0}\end{aligned} \tag{69}$$

and

$$f_4(X_0) = -\tfrac{7}{2} f_1(X_0) + \tfrac{1}{4}\tanh X_0 (3 - 2 \text{ sech}^2 X_0). \tag{70}$$

The function $J_1(X_0)$ is given by integral (13) with $n=1$. One can show that $f_3(X_0)$ is an even function and $f_4(X_0)$ is odd.

We note a quasisecular term $(9H^2 - 3|A|^2)X_0 \text{ sech}^2 X_0$ in Eq. (67); this term does not lead to the nonuniformity of the expansion as it can be incorporated in the variable width of the kink [see Eq. (80) below].

The partial differential equation arising at the order ϵ^3 is Eq. (16) with F_3 given by

$$\begin{aligned}F_3 = {} & (\partial_0\partial_1 - D_0 D_1)\phi_2 + (\partial_0\partial_2 - D_0 D_2)\phi_1 + \tfrac{1}{2}(\partial_1^2 - D_1^2)\phi_1 - \phi_1^3 \\ & - 6\phi_0\phi_1\phi_2 + V D_0\partial_0\phi_1 + \tfrac{1}{2} D_1 V \partial_0\phi_0 - \Gamma D_0\phi_1 - R D_0^2\phi_1.\end{aligned}$$

The solvability conditions give rise to amplitude equations

$$D_1 V = 0 \tag{71}$$

for the zeroth harmonic and

$$\begin{aligned}& D_2 A + \Gamma A + i\omega_0 R A - \tfrac{1}{2} i\omega_0 \zeta |A|^2 A - \tfrac{3}{4}\pi V H \\ & + \tfrac{1}{2} i\omega_0 \nu H^2 A + \tfrac{1}{2} i\omega_0 \mu H^2 A^* = 0\end{aligned} \tag{72}$$

for the first harmonic. In Eq. (72), we have introduced

$$\begin{aligned}\nu = \int_{-\infty}^{\infty} \text{sech } X_0 \tanh X_0 \, & [-6 \tanh X_0 (1 - 2 \text{ sech}^2 X_0) f_3(X_0) \\ & - 6 \text{ sech } X_0 \tanh^2 X_0 (9X_0 \text{ sech}^2 X_0 - 3 \tanh X_0 \\ & - 8 \text{ sech}^2 X_0 \tanh X_0) \\ & + 24 \tanh X_0 (\text{sech } X_0 + \text{sech}^3 X_0)(1 - 2 \text{ sech}^2 X_0) \\ & - 6 \text{ sech } X_0 \tanh X_0 (1 - 2 \text{ sech}^2 X_0)^2] dX_0,\end{aligned}$$

and

$$\begin{aligned}\mu = \int_{-\infty}^{\infty} & \text{sech } X_0 \tanh X_0 \\ & \times [24 \tanh X_0 (1 - 2 \text{ sech}^2 X_0)(\text{sech } X_0 + \text{sech}^3 X_0) \\ & - 3 \text{ sech } X_0 \tanh X_0 (1 - 2 \text{ sech}^2 X_0)^2 \\ & - 6 \text{ sech } X_0 \tanh^2 X_0 f_4(X_0)] d X_0.\end{aligned}$$

Numerically,

$$\nu = 4.159 - i\, 0.3258, \quad \mu = 1.022 + i\, 0.1623.$$

We note that the velocity enters the amplitude equation (72) as a coefficient in front of one of its two driving terms. On the other hand, Eq. (71) implies that V does not tend to zero—at least on the time scale T_1. In order to check whether the velocity decays on a longer time scale and hence whether the translational motion can drive the wobbling, we take the expansion to higher orders.

The cubic correction has the form

$$\begin{aligned}\phi_3 = {} & \varphi_3^{(0)} + \varphi_3^{(1)} e^{i\omega_0 T_0} + \text{c.c.} \\ & + \varphi_3^{(2)} e^{2i\omega_0 T_0} + \text{c.c.} + \varphi_3^{(3)} e^{3i\omega_0 T_0} + \text{c.c.}\end{aligned}$$

The zeroth-harmonic component $\varphi_3^{(0)}$ is evaluated to be zero, and the coefficient of the first-harmonic component is

$$\begin{aligned}\varphi_3^{(1)} = {} & |A|^2 A u_d(X_0) - (\partial_2 A + i\omega_0 V A) X_0 \text{ sech } X_0 \tanh X_0 \\ & + i\omega_0 V H u_1(X_0) + H|A|^2 u_2(X_0) + H A^2 u_3(X_0) \\ & + H A^2 u_4(X_0) - \tfrac{2}{3} i\omega_0 (\Gamma + i\omega_0 R)(3 - 4 \text{ sech}^2 X_0) \\ & + H^2 A u_5(X_0) + H^2 A^* u_6(X_0) + H^3 u_7(X_0).\end{aligned} \tag{73}$$

Here $u_d(X_0)$ was defined in the previous section as the bounded solution of Eq. (54), and the functions $u_n(X_0)$ $(n = 1, \ldots, 7)$ are the bounded solutions of the following nonhomogeneous equations:

$$(\mathcal{L} - 3/2)u_1 = -4 \text{ sech}^2 X_0 \tanh X_0 + \frac{3\pi}{4} \text{sech } X_0 \tanh X_0,$$

$$\begin{aligned}(\mathcal{L} - 3/2)u_2 = {} & -6 \text{ sech}^2 X_0 \tanh^2 X_0 (1 - 2 \text{ sech}^2 X_0) \\ & + 24 \text{ sech}^2 X_0 \tanh^2 X_0 (1 + \text{sech}^2 X_0) \\ & - 6 \text{ sech}^2 X_0 \tanh X_0 (2 \tanh X_0 - 3X_0) \\ & \times (1 - 2 \text{ sech}^2 X_0) \\ & - 6 \text{ sech } X_0 \tanh^2 X_0 f_3(X_0),\end{aligned}$$

$$(\mathcal{L}-3/2)u_3 = 3\,\mathrm{sech}^2 X_0 \tanh^2 X_0 (7+10\,\mathrm{sech}^2 X_0) + 12\,\mathrm{sech}^2 X_0 \tanh X_0 f_1(X_0),$$

$$(\mathcal{L}-3/2)u_4 = -6\tanh X_0 f_1(X_0),$$

$$(\mathcal{L}-3/2)u_5 = -6\tanh X_0 (1-2\,\mathrm{sech}^2 X_0) f_3(X_0) + 24\,\mathrm{sech}\, X_0 \tanh X_0 (1+\mathrm{sech}^2 X_0) \times (1-2\,\mathrm{sech}^2 X_0) - 6\,\mathrm{sech}\, X_0 \tanh^2 X_0 (9X_0\,\mathrm{sech}^2 X_0 - 3\tanh X_0 - 8\,\mathrm{sech}^2 X_0 \tanh X_0) - 6\,\mathrm{sech}\, X_0 \tanh X_0 \times (1-2\,\mathrm{sech}^2 X_0)^2 - \tfrac{3}{2}\nu\,\mathrm{sech}\, X_0 \tanh X_0,$$

$$(\mathcal{L}-3/2)u_6 = -6\,\mathrm{sech}\, X_0 \tanh^2 X_0 f_4(X_0) + 24\,\mathrm{sech}\, X_0 \tanh X_0 (1+\mathrm{sech}^2 X_0) \times (1-2\,\mathrm{sech}^2 X_0) - 3\,\mathrm{sech}\, X_0 \tanh X_0 \times (1-2\,\mathrm{sech}^2 X_0)^2 - \tfrac{3}{2}\mu\,\mathrm{sech}\, X_0 \tanh X_0,$$

and

$$(\mathcal{L}-3/2)u_7 = -6\tanh X_0 (1-2\,\mathrm{sech}^2 X_0) f_4(X_0) - 3(1-2\,\mathrm{sech}^2 X_0)^3 - 6\,\mathrm{sech}\, X_0 \tanh^2 X_0 (9X_0\,\mathrm{sech}^2 X_0 - 3\tanh X_0 - 8\,\mathrm{sech}^2 X_0 \tanh X_0).$$

Like the functions u_d and u_e of the previous section, the solutions $u_n(X_0)$ are defined up to the addition of a multiple of y_w. As in the previous section, this does not provide any extra degrees of freedom and the multiple of y_w cancels out in the integrals η and χ below. The solutions u_1, u_5, and u_6 are odd, while u_2, u_3, u_4, and u_7 can be chosen to be even functions. The only fact about u_1 that we need is that it is a real solution; owing to its reality, u_1 does not contribute to the solvability conditions below. The solutions $u_n(X_0)$ with $n=2,\ldots,7$ are determined using the variation of parameters and numerical integration.

To eliminate the quasisecular term proportional to $X_0\,\mathrm{sech}\, X_0 \tanh X_0$ in Eq. (73), we set $\partial_2 A = -i\omega_0 V A$.

It is not necessary to calculate the second- and the third-harmonic components, $\varphi_3^{(2)}$ and $\varphi_3^{(3)}$, as these do not contribute to the zeroth harmonic at fourth order in ϵ, where the leading-order behavior of V will reveal itself. The equation arising at $\mathcal{O}(\epsilon^4)$ is Eq. (55), with

$$F_4 = (\partial_0\partial_1 - D_0D_1)\phi_3 + (\partial_0\partial_2 - D_0D_2)\phi_2 + \tfrac{1}{2}(\partial_1^2 - D_1^2)\phi_2 + (\partial_0\partial_3 - D_0D_3)\phi_1 + (\partial_1\partial_2 - D_1D_2)\phi_1 - 3\phi_1^2\phi_2 - 6\phi_0\phi_1\phi_3 - 3\phi_0\phi_2^2 + VD_0\partial_0\phi_2 + VD_0\partial_1\phi_1 + \tfrac{1}{2}D_2V\partial_0\phi_0 - \tfrac{1}{2}V^2\partial_0^2\phi_0 - RD_0^2\phi_2 - \Gamma D_0\phi_2 + \Gamma V\partial_0\phi_0.$$

The solvability condition for the zeroth harmonic yields

$$D_2V = -2\Gamma V - \frac{3}{2}\eta H|A|^2A + \text{c.c.} - \frac{3}{2}\chi H^3A + \text{c.c.} + \frac{3\pi}{4}i\omega_0 H(\Gamma - i\omega_0 R)A + \text{c.c.}, \tag{74}$$

where

$$\eta = \int_{-\infty}^{\infty} \mathrm{sech}^2 X_0 [24\,\mathrm{sech}^2 X_0 \tanh^2 X_0 (\mathrm{sech}\, X_0 + \mathrm{sech}^3 X_0) - 3\,\mathrm{sech}^2 X_0 \tanh^2 X_0 f_3^*(X_0) - 6\,\mathrm{sech}^3 X_0 \tanh X_0 (2\tanh X_0 - 3X_0)(1-2\,\mathrm{sech}^2 X_0) - 6\,\mathrm{sech}\, X_0 \tanh X_0 (1-2\,\mathrm{sech}^2 X_0) f_1(X_0) - 6\,\mathrm{sech}\, X_0 \tanh^2 X_0 u_3(X_0) - 6\,\mathrm{sech}\, X_0 \tanh^2 X_0 u_4(X_0) - 6\,\mathrm{sech}\, X_0 \tanh^2 X_0 u_2^*(X_0) + 24\,\mathrm{sech}^2 X_0 \tanh X_0 (2\tanh X_0 - 3X_0) \times (\mathrm{sech}\, X_0 + \mathrm{sech}^3 X_0) - 6\tanh X_0 (1-2\,\mathrm{sech}^2 X_0) u_d(X_0) - 6\tanh X_0 f_1(X_0) f_3^*(X_0)]\, dX_0,$$

and

$$\chi = \int_{-\infty}^{\infty} \mathrm{sech}^2 X_0 [-6\,\mathrm{sech}\, X_0 \tanh^2 X_0 u_7^*(X_0) - 6\tanh X_0 (1-2\,\mathrm{sech}^2 X_0) u_5(X_0) - 6\tanh X_0 (1-2\,\mathrm{sech}^2 X_0) u_6^*(X_0) + 24(1-2\,\mathrm{sech}^2 X_0)^2 (\mathrm{sech}\, X_0 + \mathrm{sech}^3 X_0) + 18\,\mathrm{sech}\, X_0 \tanh X_0 (1+2\,\mathrm{sech}^2 X_0)(9X_0\,\mathrm{sech}^2 X_0 - 3\tanh X_0 - 8\,\mathrm{sech}^2 X_0 \tanh X_0) - 3(1-2\,\mathrm{sech}^2 X_0)^2 f_3(X_0) - 6\tanh X_0 f_3(X_0) f_4^*(X_0) - 6\,\mathrm{sech}\, X_0 \tanh X_0 (1-2\,\mathrm{sech}^2 X_0) f_4^*(X_0)]\, dX_0.$$

Numerically,

$$\eta = -2.005 - i\,0.3823, \quad \chi = -12.21 - i\,0.5706.$$

Writing $a=\epsilon A$ as before, and combining $D_1A=0$ with Eq. (72) with the help of the chain rule, we obtain the amplitude equation in terms of the unscaled parameters,

$$\dot{a} = -\gamma a - i\omega_0\rho a + \frac{1}{2}i\omega_0\zeta|a|^2a + \frac{3\pi}{4}vh - \frac{1}{2}i\omega_0\nu h^2 a - \frac{1}{2}i\omega_0\mu h^2 a^* + \mathcal{O}(|a|^5). \tag{75a}$$

Similarly, combining Eq. (71) with Eq. (74), we arrive at

$$\dot{v} = -2\gamma v - \frac{3}{2}\eta h|a|^2a + \text{c.c.} - \frac{3}{2}\chi h^3 a + \text{c.c.} + \frac{3\pi}{4}i\omega_0 h(\gamma - i\omega_0\rho)a + \text{c.c.} + \mathcal{O}(|a|^5). \tag{75b}$$

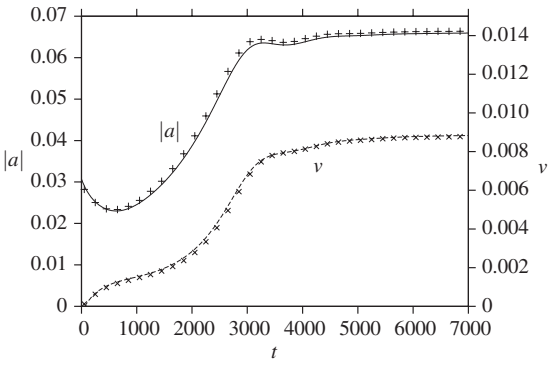

FIG. 4. An example of the kink being accelerated by the 1:1 direct driving. Here $h=0.012$, $\gamma=1\times10^{-3}$, and $\rho=0$. The crosses are measured values from numerical simulations of the original partial differential equation (63), while the lines are the predictions of the amplitude equations (75).

B. Reduced dynamics in three dimensions

Thanks to the a-dependent driving terms in Eq. (75b), the direct driving can sustain the translational motion of the kink, in contrast to the parametrically driven cases we have considered. Figure 4 shows an example of the kink accelerated by the 1:1 direct driving force which simultaneously excites the wobbling. Note that results from the three-dimensional system (75) are in excellent agreement with predictions of the full partial differential equation — not only after the dynamics have settled to a stationary regime but also during the transient phase.

The detailed analysis of the three-dimensional system (75) will be reported elsewhere; here, we limit ourselves to several basic observations. Firstly, it is straightforward to see that, when $h=0$, the trivial fixed point $a=v=0$ is the only attractor available in the system. Secondly, numerical simulations of the three-dimensional system show that as h is increased for fixed γ and ρ, a nontrivial fixed point bifurcates from the point $a=v=0$ [see Figs. 5(a) and 5(b)]. For lower values of ρ, the bifurcation is subcritical (as in the case shown in Fig. 5); for higher ρ, it is supercritical. As h approaches some critical driving strength h_c, both the $|a|$ and the v components of the nontrivial fixed point tend to infinity. Finally, in the region $h>h_c$, there are no stable fixed points. In this region, simulations of system (75) reveal a blowup regime, where the functions $|a(t)|, v(t)$ grow without bounds.

To determine the critical value h_c, we assume that the blowup regime is self-similar, that is, that the growth of v is pegged to that of a. This assumption can be formalized by expanding v and $\mathrm{Arg}(a)$ in powers of large $|a|$ as follows:

$$v = V_3|a|^3 + V_1|a| + V_{-1}|a|^{-1} + \cdots, \tag{76a}$$

$$a = |a|e^{-i\theta}, \quad \theta = \theta_0 + \theta_{-2}|a|^{-2} + \theta_{-4}|a|^{-4} + \cdots. \tag{76b}$$

Substituting these expansions in Eqs. (75a) and (75b) and equating coefficients of like powers of $|a|$ to zero, we can evaluate the coefficients V_n and θ_n to any order—this justifies the assumption.

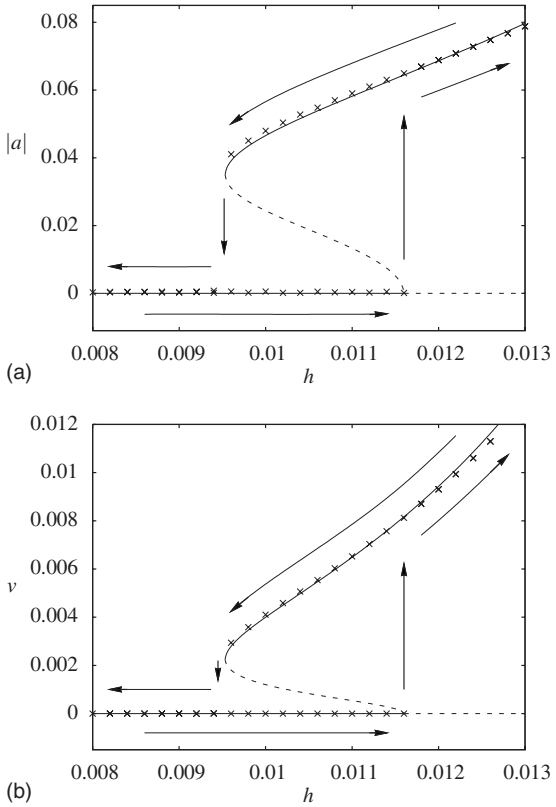

FIG. 5. The hysteresis loop in the 1:1 directly driven ϕ^4 equation with $\gamma=10^{-3}$ and $\rho=-10^{-4}$. The driving strength is increased from $h=8\times10^{-3}$ to 13×10^{-3} in increments of 0.2×10^{-3} and then reduced back to 8×10^{-3}. The "crosses" are measured values from numerical simulations of the partial differential equation (63) whereas the continuous and the dashed lines show the stable and the unstable fixed points of the amplitude equations (75).

In particular, setting to zero the coefficients of $|a|^3$ in Eq. (75a) gives

$$e^{i\theta_0} = -i\frac{\zeta}{|\zeta|}, \quad V_3 = \frac{2\omega_0|\zeta|}{3\pi}\frac{1}{h}. \tag{77}$$

On the other hand, substituting Eqs. (76) in Eq. (75b), we get an equation describing the growth of $|a(t)|$,

$$\frac{d}{dt}|a| = \mathfrak{r}|a| + \mathcal{O}(|a|^{-1}),$$

where the growth rate

$$\mathfrak{r} = -\frac{2}{3}\gamma - \frac{\eta e^{-i\theta_0} + \eta^* e^{i\theta_0}}{2}\frac{h}{V_3}.$$

Substituting for $e^{i\theta_0}$ and V_3 from Eq. (77), this becomes

$$\mathfrak{r} = -\frac{2}{3}\gamma - \frac{3\pi}{2\omega_0|\zeta|}\frac{\eta e^{-i\theta_0} + \eta^* e^{i\theta_0}}{2}h^2. \tag{78}$$

The growth of $|a|$ is due to the h^2 term in Eq. (78) which has a positive coefficient; the growth is damped by the γ term. If we reduce h keeping γ fixed, then, at $h=h_c$ where

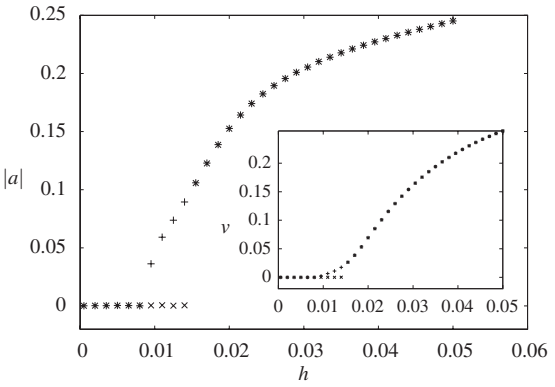

FIG. 6. Results of numerical simulations of Eq. (63) with h raised beyond the critical value $h_c=0.021$. As in Fig. 5, in this plot $\gamma=10^{-3}$ and $\rho=-10^{-4}$. The main panel shows values of $|a|$ and the inset values of v as a function of h. The "crosses" represent measurements obtained as h is increased from 0.0005 to 0.05 in steps of 1.5×10^{-3}; the "pluses" are obtained as h is decreased back to 0.0005. An "asterisk" results when a "plus" is superimposed over the "cross" at the same point.

$$h_c=\left[\frac{8\omega_0}{9\pi}\frac{|\zeta|^2}{i(\zeta\eta^*-\zeta^*\eta)}\right]^{1/2}\gamma^{1/2}=0.6523\gamma^{1/2}, \qquad (79)$$

the growth rate will become equal to zero. At this point the blowup regime is replaced with a stable fixed point—which, however, still has large values of $|a|$ and v. [Reducing h further, the fixed point will persist but the similarity relations (76) will no longer be valid.] Note that the critical value (79) does not depend on ρ. Numerical simulations of Eqs. (75) carried out for a variety of γ and ρ reproduce this value of h_c to a high accuracy.

As h is increased toward h_c and neither $|a|$ nor v component of the stationary point is small any longer, system (75) ceases to provide any reliable description for the dynamics of the wobbler. A natural question that arises here is what dynamical regime the kink settles to for h just below h_c and for h above h_c. In other words, we want to know what happens when the wobbler is driven with the small strength h of order $\gamma^{1/2}$ [so that conditions (64) are still in place] for which our finite-dimensional approximation is no longer valid. To answer this, we have conducted a series of numerical simulations of Eq. (63) with h raised from $h<h_c$ to $h>h_c$. The simulations reveal that in the region inaccessible to our finite-dimensional approximation, the kink settles to wobbling with a constant amplitude, which is accompanied by its translational motion with a constant velocity (see Fig. 6). The numerically detected values of a and v are of order $\gamma^{1/3}$ in this region; this accounts for the inadequacy of our approximation, which was based on the assumptions $a=\mathcal{O}(\gamma^{1/2})$ and $v=\mathcal{O}(\gamma)$.

The behavior of the 1:1 externally driven wobbling kink above (and just below) the critical value is an issue to which we are planning to return in the near future. To derive the correct set of amplitude equations, we will need to use our asymptotic approach with modified scalings for a and v.

C. 1:1 directly driven wobbler and its radiation

Up to $\mathcal{O}(\epsilon^2)$, the perturbation expansion gives

$$\begin{aligned}\phi(x,t)=&\tanh[(1-3|a|^2+9h^2)\xi]+[a\ \mathrm{sech}\ \xi\tanh\xi\\&+h(1-2\ \mathrm{sech}^2\ \xi)]\,e^{i\Omega t}+\mathrm{c.c.}+2|a|^2\mathrm{sech}^2\,\xi\tanh\xi\\&-4h(a+a^*)\ \mathrm{sech}\,\xi(1+\mathrm{sech}^2\ \xi)\\&-h^2(3\tanh\xi+8\ \mathrm{sech}^2\ \xi\tanh\xi)\\&+[a^2f_1(\xi)+haf_3(\xi)+h^2f_4(\xi)]\,e^{2i\Omega t}+\mathrm{c.c.}+\mathcal{O}(|a|^3).\end{aligned} \qquad (80)$$

For sufficiently large t, the variable ξ is given by $x-vt-x_0$, where x_0 is determined by the initial conditions. The complex constant a and the real v are components of a stable fixed point (trivial or nontrivial) of system (75). The functions f_1, f_3, and f_4 are given by Eqs. (12), (69), and (70). As in all previously considered driving regimes, the 1:1 direct driver excites a standing wave with the amplitude proportional to the driver's strength and frequency equal to the frequency of the driving [first two terms in the second line in Eq. (80)]. The standing wave includes also the second and the zeroth harmonics, both with the amplitudes of order h^2 (terms in the fourth and the last line).

Like the expansions in the previous sections, Eq. (80) is only valid at distances $|\xi|=\mathcal{O}(1)$. To describe the waveform at longer distances, we consider the outer expansions

$$\phi=\ \pm\ 1+\epsilon(He^{i\omega_0T_0}+\mathrm{c.c.})+\epsilon^2\phi_2+\epsilon^3\phi_3+\cdots$$

in the regions $X_0>0$ and $X_0<0$, respectively. Substituting in Eq. (65), the order ϵ^2 gives

$$\phi_2=\ \mp\ 3H^2\pm\tfrac{3}{4}H^2e^{2i\omega_0T_0}+\mathrm{c.c.}+\mathcal{J}_\pm B_\pm e^{i(\omega_\pm T_0-k_\pm X_0)}+\mathrm{c.c.} \qquad (81)$$

Here the top and the bottom signs pertain to the $X_0>0$ and the $X_0<0$ regions, respectively. The amplitudes $B_\pm$ are functions of the slow variables: $B_\pm=B_\pm(X_1,\ldots;T_1,\ldots)$ and the normalization coefficients $\mathcal{J}_\pm$ have been introduced for later convenience. Matching the outer solution (81) to the inner solution (9) with coefficients as in Eqs. (66)–(68), and choosing $\mathcal{J}_\pm=\pm(2-ik_0)$, we obtain $\omega_\pm=2\omega_0$, $k_\pm=\pm k_0$, and

$$\begin{aligned}&B_\pm(0,0,\ldots;T_1,T_2,\ldots)\\&\quad=\tfrac{1}{8}J_2^\infty\left[A^2(0,0,\ldots;T_2,T_3,\ldots)-\tfrac{7}{2}H^2\right]\\&\qquad\pm i\tfrac{15}{32}k_0J_1^\infty HA(0,0,\ldots;T_2,T_3,\ldots).\end{aligned} \qquad (82)$$

Equations (82) are the boundary conditions for the amplitude fields B_+ and B_-. The equations of motion for these fields are obtained at the order ϵ^3 of the outer expansion. Namely, the solvability conditions for $\varphi_3^{(2)}$, the coefficient of the second harmonic at the order ϵ^3, give

$$D_1B_++c_0\partial_1B_+=0,\quad X_1>0, \qquad (83a)$$

$$D_1B_--c_0\partial_1B_-=0,\quad X_1<0, \qquad (83b)$$

where $c_0=k_0/(2\omega_0)$.

As before, the analysis of the linear transport equations (83) under the boundary conditions (82) is straightforward. The initial condition $B_+(X_1,\ldots;0,\ldots)$ defined in $X_1>0$, propagates unchanged to the right and the initial condition $B_-(X_1,\ldots;0,\ldots)$ defined in $X_1<0$, propagates unchanged to

the left, both with the velocity c_0. In the expanding region $-c_0T_1<X_1<c_0T_1$, the amplitudes $B_{\pm}$ are constants defined by conditions (82). In terms of the second-harmonic radiation, this corresponds to two groups of radiation waves, diverging to the left and to the right and leaving a sinusoidal waveform of constant amplitude in between.

D. Qualitative analysis

The reason why the external force does not couple directly to the wobbling mode in the case of the 1:1 external driving (as it did in the case of the 1:1 *parametric* resonance) is the discrepancy in the parity of the driving profile and the wobbling mode. Instead, there are three indirect amplification mechanisms at work in this case. In each of these, the central role is played by the even-parity standing wave excited by the driver. Firstly, the square of this standing wave couples to the wobbling mode via the term $\epsilon^3\phi_1^3$. Secondly, the second and the zeroth harmonics of the standing wave as well as the second-harmonic radiation excited by the standing wave couple to the wobbling mode via the term $\epsilon^3\phi_0\phi_1\phi_2$. Thirdly, when the kink moves relative to the standing wave, the odd-parity wobbling mode acquires an even-parity component which then couples to the standing wave. [This process is accounted for by the term $\epsilon^3VD_0\partial_0\phi_1$ in Eq. (65).] Since the first two mechanisms rely upon a quadratic superharmonic of the induced standing wave (with the amplitude of the superharmonic being proportional to h^2), and since the velocity of the kink (which determines the amplitude of the even component of the wobbling mode in the third mechanism) is small, the 1:1 direct resonance is weak.

VII. CONCLUDING REMARKS

In this paper, we have used the asymptotic method to study the wobbling kink driven by four types of resonant driving force, viz., the 1:1 and 2:1 parametric and 1:2 and 1:1 external driving. We have demonstrated the existence of resonance (i.e., the existence of sustained wobbling with nondecaying amplitude despite losing energy to radiation and dissipation) in all four cases. This conclusion (verified in direct numerical simulations of the corresponding partial differential equation) agrees with results of Quintero *et al.* who also demonstrated the existence of the resonance in the 1:1 parametrically and 1:2 directly driven ϕ^4 equations [2–4]. However, we are in disagreement with these authors on the 1:1 directly driven, damped equation. Namely, our method does capture the resonance in this case, whereas their collective-coordinate approach does not. (In fairness to the pioneering work of Quintero *et al.*, their direct numerical simulations did reveal a resonant peak at the frequency of the driver equal to the natural wobbling frequency of the kink—an experimental result which, however, did not reconcile with their collective-coordinate predictions [2,3].)

In each of the four driving regimes that we have considered in this paper, we have derived a system of equations for the complex amplitude of the wobbling coupled to the velocity of the kink. The predictions based on this dynamical system are in agreement with results of the direct numerical simulation of the full partial differential equation. In three out of four cases considered, the velocity of the kink is shown to decay to zero as time advances, as a result of which the dimension of this dynamical system reduces from 3 to 2. Only in one case (the case of the 1:1 directly driven wobbler) does the velocity of the kink not necessarily decay to zero. In this latter case the wobbling of the kink is accompanied by its motion with nonzero velocity.

Each of the four dynamical systems derived here gives rise to a bifurcation diagram featuring bistability and hysteretical transitions in the wobbling amplitude. In the 1:1 parametric and the 1:2 direct resonances, the bistability is between two nonzero values of the wobbling amplitude, whereas in the 2:1 parametrically and the 1:1 directly driven ϕ^4 equations, one of the two stable regimes involves a nonzero and the other one involves a zero amplitude. It is fitting to note here that the collective-coordinate approach [2–4] does not capture the bistability and the hysteresis.

In Sec. IV, we ranked the two parametric resonances according to the amplitude of the stationary wobbling resulting from the driving with a certain reference strength h. Adding to this hierarchy the two direct resonances produces the following ranking. The 1:1 parametric resonance is the strongest of the four cases; in this case, the amplitude of the stationary wobbling, a is of order $h^{1/3}$. The 2:1 parametric resonance is the second strongest; in this case, the kink responds with the wobbling amplitude $a\sim h^{1/2}$. The 1:2 direct resonance has $a\sim h^{2/3}$ and the 1:1 direct resonance is the weakest: $a\sim h$. (The fact that the harmonic direct resonance is weaker than the superharmonic one is in agreement with results of [2,3] where it was established in the undamped situation.)

Our asymptotic approach also allows one to rank the resonances according to the widths of the corresponding Arnold tongues on the "driving strength vs driving frequency" plane. The 1:1 parametric resonance is the widest one; in this case, the resonant region is bounded by the curve $h\sim\rho^{3/2}$. The 2:1 parametric resonance is the second widest; in this case, the Arnold tongue has $h\sim\rho$. The 1:2 direct resonance has $h\sim\rho^{3/4}$ and the 1:1 direct resonance is the narrowest: $h\sim\rho^{1/2}$. We should also mention that the 1:1 parametric and the 1:2 direct resonances have no threshold in the strength of the driver, whereas the 2:1 parametric and 1:1 direct resonances occur only if the driving strength exceeds a certain threshold value.

ACKNOWLEDGMENTS

We thank Alan Champneys for useful remarks. O.F.O. was supported by funds provided by the National Research Foundation of South Africa and the University of Cape Town. I.V.B. was supported by the NRF under Grant No. 2053723.

[1] J. A. González, B. A. Mello, L. I. Reyes, and L. E. Guerrero, Phys. Rev. Lett. **80**, 1361 (1998).
[2] N. R. Quintero, A. Sánchez, and F. G. Mertens, Phys. Rev. Lett. **84**, 871 (2000).
[3] N. R. Quintero, A. Sánchez, and F. G. Mertens, Phys. Rev. E **62**, 5695 (2000).
[4] N. R. Quintero, A. Sánchez, and F. G. Mertens, Phys. Rev. E **64**, 046601 (2001).
[5] Yu. S. Kivshar, A. Sánchez, and L. Vázquez, Phys. Rev. A **45**, 1207 (1992).
[6] Zhang Fei, V. V. Konotop, M. Peyrard, and L. Vázquez, Phys. Rev. E **48**, 548 (1993).
[7] F. G. Bass, Yu. S. Kivshar, V. K. Konotop, and Yu. A. Sinitsyn, Phys. Rep. **157**, 63 (1988); M. J. Rodríguez-Plaza and L. Vázquez, Phys. Rev. B **41**, 11437 (1990); E. Moro and G. Lythe, Phys. Rev. E **59**, R1303 (1999); S. Habib and G. Lythe, Phys. Rev. Lett. **84**, 1070 (2000); the overdamped limit was considered by G. Lythe and S. Habib, Comput. Sci. Eng. **8**, 10 (2006); G. Lythe and F. G. Mertens, Phys. Rev. E **67**, 027601 (2003).
[8] A. L. Sukstanskii and K. I. Primak, Phys. Rev. Lett. **75**, 3029 (1995).
[9] M. Borromeo and F. Marchesoni, Chaos **15**, 026110 (2005).
[10] L. Morales-Molina, F. G. Mertens, and A. Sánchez, Phys. Rev. E **72**, 016612 (2005).
[11] L. Morales-Molina, N. R. Quintero, A. Sánchez, and F. G. Mertens, Chaos **16**, 013117 (2006).
[12] P. Laguna and W. H. Zurek, Phys. Rev. Lett. **78**, 2519 (1997); Phys. Rev. D **58**, 085021 (1998); J. Dziarmaga, P. Laguna, and W. H. Zurek, Phys. Rev. Lett. **82**, 4749 (1999).
[13] F. Marchesoni, L. Gammaitoni, and A. R. Bulsara, Phys. Rev. Lett. **76**, 2609 (1996).
[14] Yu. S. Kivshar and A. Sánchez, Phys. Rev. Lett. **77**, 582 (1996); A. L. Sukstanskii and K. I. Primak, *ibid.* **77**, 583 (1996).
[15] M. J. Rice and E. J. Mele, Solid State Commun. **35**, 487 (1980).
[16] M. J. Rice, Phys. Rev. B **28**, 3587 (1983).
[17] I. V. Barashenkov, N. V. Alexeeva, and E. V. Zemlyanaya, Phys. Rev. Lett. **89**, 104101 (2002); N. V. Alexeeva, Theor. Math. Phys. **144**, 1075 (2005); I. V. Barashenkov, S. R. Woodford, and E. V. Zemlyanaya, Phys. Rev. E **75**, 026604 (2007).
[18] I. V. Barashenkov and O. F. Oxtoby, **80**, 026608 (2009), the preceding paper.
[19] R. Grimshaw, *Nonlinear Ordinary Differential Equations* (Blackwell Scientific Publications, Oxford, 1990).
[20] I. V. Barashenkov, M. M. Bogdan, and V. I. Korobov, EPL **15**, 113 (1991).
[21] H. Segur, J. Math. Phys. **24**, 1439 (1983).